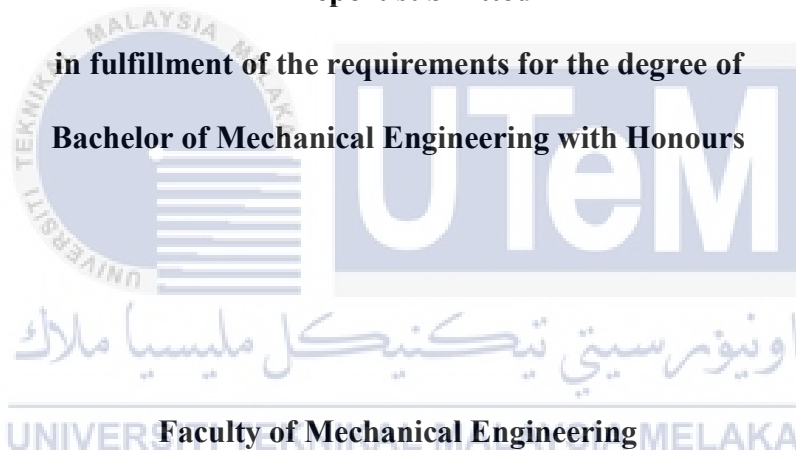


**FORCE CONVECTION FLOW AND THERMAL ANALYSIS IN COMPOSITE
CURING AUTOCLAVE**

WONG YONG HAN

A report submitted

**in fulfillment of the requirements for the degree of
Bachelor of Mechanical Engineering with Honours**



UNIVERSITI TEKNIKAL MALAYSIA MELAKA

2019

DECLARATION



I declare that this project report entitled “Force Convection Flow and Thermal Analysis in Composite Curing Autoclave” is the result of my own work except as cited in the references.


Signature	:	
Name	:	WONG YONG HAN
Date	:	25/6/19

اونیورسیتی تکنیکل ملیسیا ملاک
UNIVERSITI TEKNIKAL MALAYSIA MELAKA

APPROVAL

I hereby declare that I have read this project report and in my opinion this report is sufficient in terms of scope and quality for the award of the degree of Bachelor of Mechanical Engineering with Honours.



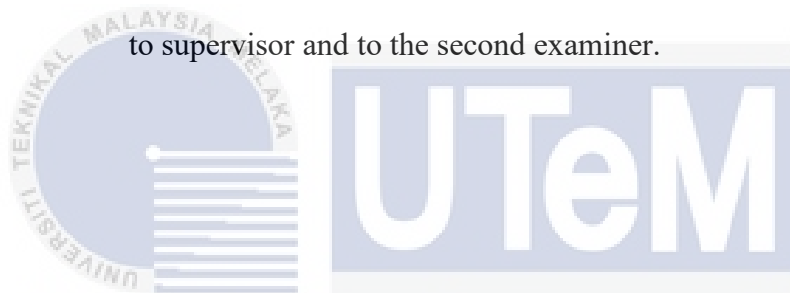
Signature : 

Supervisor's Name : **DR. ERNIE BINTI MAT TOKIT**
PENSYARAH KANAN
FAKULTI KEJURUTERAAN MEKANIKAL
UNIVERSITI TEKNIKAL MALAYSIA MELAKA

Date : 25/6/19

SUPERVISOR'S DECLARATION

I have checked this report and the report can now be submitted to JK-PSM to be delivered back to supervisor and to the second examiner.



Signature
اونيورسي تيكنيكل مليسيا ملاك

Name of Supervisor
UNIVERSITI TEKNIKAL MALAYSIA MELAKA

Date :.....

ABSTRACT

An autoclave was a sealed welly container which used for the process involved high temperature and pressure. Past researches focused on the efficiency of autoclave by reduction of cycle time and other properties. This project aimed to investigate the velocity and temperature distribution inside the autoclave, determined the suitable fan and heater position for uniform velocity and temperature distribution inside the autoclave. To illustrate the velocity and temperature distribution inside the autoclave, CFD simulation apps such as Computational Fluid Dynamic, FLUENT ANSYS was used. From the result gained from simulations, the required parameter that velocity distribution for achieving the uniform flow was 1m/s. While the temperature distribution was in stable that surrounded the mold with the required velocity of air flow above 1m/s. From the comparison of different velocities towards each temperature distribution, the recommended was air with 1m/s velocity.

ABSTRAK

Autoklaf adalah wadah penyerlah yang digunakan untuk proses yang melibatkan suhu dan tekanan tinggi. Penyelidikan yang lalu memberi tumpuan kepada kecekapan autoklaf oleh pengurangan masa kitaran dan sifat-sifat lain. Projek ini bertujuan untuk menyiasat pengedaran halaju dan suhu di dalam autoklaf, menentukan kedudukan kipas dan pemanas yang sesuai untuk halaju seragam dan pengedaran suhu di dalam autoklaf. Untuk menggambarkan halaju dan pengedaran suhu di dalam autoklaf, aplikasi simulasi CFD seperti Computational Fluid Dynamic, FLUENT ANSYS telah digunakan. Daripada hasil yang diperolehi dari simulasi, parameter yang diperlukan bahawa pengagihan halaju untuk mencapai aliran seragam adalah 1m/s. Walaupun pengedaran suhu berada dalam keadaan stabil yang mengelilingi acuan dengan halaju yang diperlukan aliran udara di atas 1m/s. Daripada perbandingan halaju yang berbeza ke arah setiap pengagihan suhu, yang dicadangkan adalah udara dengan halaju 1m/s.

ACKNOWLEDGEMENT

I would like to express my sincere appreciation towards my supervisor, Dr Ernie Binti Mat Tokit. She has guide me along the whole PSM 1 from start to the end and share her knowledge on how to do the CFD simulation and project report writing skills. I would also like wish to extend my gratitude towards my housemates who help me in software technics and share their information about the PSM project with me.

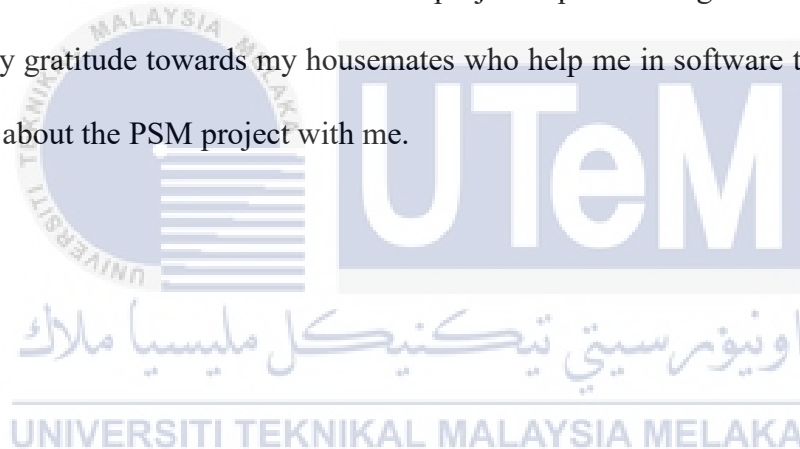



TABLE OF CONTENT

CHAPTER	CONTENT	PAGE
	SUPERVISOR'S DECLARATION	i
	ABSTRACT	ii
	ABSTRACK	iii
	ACKNOWLEDGMENT	iv
	TABLE OF CONTENT	v
	LIST OF FIGURES	viii
	LIST OF TABLES	xi
	LIST OF ABBREVIATIONS	xii
	LIST OF SYMBOLS	xiii
CHAPTER 1	INTRODUCTION	1
	1.0 BACKGROUND	1
	1.1 PROBLEM STATEMENT	3
	1.2 OBJECTIVES	4
	1.3 SCOPE	4
CHAPTER 2	LITERATURE REVIEW	5

2.1	THE CONCEPT OF OVENS AND AUTOCLAVES	5
2.2	FLOW VISUALIZATION OF OVENS AND AUTOCLAVES	9
2.3	TEMPERATURE DISTRIBUTION OF OVENS AND AUTOCLAVES	15
2.4	CURRENT DESIGN IN OPTIMIZE THE PERFORMANCE IN BOTH OVENS AND AUTOCLAVES	18
CHAPTER 3	METHODOLOGY	20
3.2.0	NUMERICAL WORK	22
3.2.1	MODEL THE DOMAIN	24
3.2.2	MESHING TYPE	25
3.2.3	MATERIAL PROPERTIES SET-UP	26
3.2.4	BOUNDARY CONDITION SET-UP	27
3.2.5	RUN THE SOLVER	28
3.2.6	REDO MESHING WITH DIFFERENT PROPERTIES	28
CHAPTER 4	RESULT & DISCUSSION	29
4.1	VALIDATION TOWARDS JOURNAL	28
4.2	VERIFICATION USING DIFFERENT NUMBER OF MESHING	31

4.3	COMPARISON ANALYSIS OF BOUNDARY CONDITION OF PRESSURE OUTLET AND EXHAUST FAN	36
4.4	FLOW DISTRIBUTION AT DIFFERENT VELOCITY	38
4.5	TEMPERATURE DISTRIBUTION AT DIFFERENT VELOCITY	41
CHAPTER 5	CONCLUSION	45
5.2	RECOMMENDATION	48
	REFERENCE	49
	APPENDIX	51



اونیورسیتی تکنیکل ملیسیا ملاک
 UNIVERSITI TEKNIKAL MALAYSIA MELAKA

LIST OF FIGURES

FIGURES	DESCRIPTIONS	PAGES
Figure 2.1:	The mimic of autoclave systems	5
Figure 2.2:	The model of the sample used for validation purpose	7
Figure 2.3:	The curing process for metal specimen inside the autoclave	7
Figure 2.4:	The oven and its main parts	8
Figure 2.5:	The cross diagram of the oven and its particular usage	8
Figure 2.6:	The figure of different inlet against the heat flow pattern	9
Figure 2.7:	The air velocity flow diagram with temperature differences	10
Figure 2.8:	The flow pattern inside the oven when obstacles are placed	10
Figure 2.9:	The schematic diagram of air circulation inside an autoclave	11
Figure 2.10:	The heated air flow of a coke oven with its structure	12
Figure 2.11:	The overview of heat flow across the coke oven	13
Figure 2.12:	The air flow of the autoclave model	13
Figure 2.13:	The streamline of the symmetrical plane	14
Figure 2.14:	The velocity distribution of LDPE autoclave reactor with different impellers	14
Figure 2.15:	The streamline pattern and the present simulation	15
Figure 2.16:	The temperature field simulation inside the oven	15

Figure 2.17:	The temperature distribution of the fairing and tools at 60 minutes	16
Figure 2.18:	The temperature distribution on the surface of the model	17
Figure 2.19:	The references of conveyer belt speed	18
Figure 2.20:	The modified conveyer belt speed	19
Figure 2.21:	The improvement of cycle time as a function of different modification	19
Figure 3.1	The general methodology used	21
Figure 3.2:	a) cylinder-like autoclave model. b) combined model with brick- shape mold.	24
Figure 3.3:	The brick is moved into the center of the cylinder	24
Figure 3.4:	The final pattern of the sample inside gambit drawing	25
Figure 3.5:	The edge meshing of the sample	25
Figure 3.6:	a) The final meshing b) The examined cross-section plane skewness	26
Figure 3.7:	The material selection command to insert corresponding material	26
Figure 3.8:	The setting of pressure outlet in Boundary Condition command	27
Figure 3.9:	The iterate command in FLUENT command	28
Figure 3.10:	The number of iterations	28
Figure 4.1:	The turbulent kinetic energy of the steady-state flow of the reference	29
Figure 4.2:	The turbulent kinetic energy of the steady-state flow of the model	29
Figure 4.3:	The different design of the mold	30
Figure 4.4:	Volumetric meshing on cylindrical volume	31
Figure 4.5:	Worse meshing element occurring at aside of mold which in- contacted with cylinder volumetric mesh	32

Figure 4.6:	The geometry of the model with all represented edges' symbols	33
Figure 4.7:	Unaccepted meshing with skewness greater than 0.97	34
Figure 4.8:	The error showed after volumetric meshing with all the data in Table 4.1 on the cylinder volume	34
Figure 4.9:	Geometry without panel	34
Figure 4.10:	Comparison between boundary condition of pressure outlet and exhaust fan	36
Figure 4.11:	Velocity contour for inlet velocity of 1m/s, 2m/s, and 3m/s	38
Figure 4.12:	The red circles show the difference between three different cases	39
Figure 4.13:	Temperature contour for inlet velocity of 1m/s, 2m/s, and 3m/s	42
Figure 4.14:	Temperature contour for inlet velocity of 0.2m/s, 0.5m/s, and 1m/s	44
Figure 5.1:	The red circle is the predicted area that heater to be located	46
Figure 5.2:	The white circle is the area that blower applied, while green circle is the exhaust fan	47

LIST OF TABLES

TABLE	TITLE	PAGES
Table 4.1:	Table of numbers of nodes that applied on each particular side edge	32
Table 4.2:	Table of numbers of nodes that applied on each particular side edges for geometry without panel	34



LIST OF ABBREVIATIONS

FLUENT	Fluent-Ansys apps
CFD	Computational Fluid Dynamics
2D	Two Dimensional
3D	Three Dimensional
LDPE	Low-Density Polyethylene



LIST OF SYMBOLS

A	=	related area
ρ	=	density of fluid
u	=	velocity of fluid
L	=	characteristic linear dimension
μ	=	dynamic viscosity of fluid
ν	=	kinematic viscosity of fluid
t	=	time taken
\emptyset	=	diameter of circle
ω	=	vorticity



CHAPTER 1

INTRODUCTION

1.0 BACKGROUND

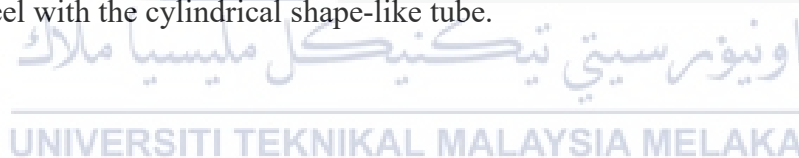
An autoclave is a pressurized chamber which used to carry out industrial processes such as curing, body piercing and other processes that required elevated temperature with different pressures. While the heat flow is the pattern of the temperature of the air that flows through the whole chamber with different temperature and velocity.

The normal dimensions of the autoclave chamber for common usage such as the cooling process for small scale, medium scale, and large-scale productions respectively. With the aids of Computational fluid dynamics (CFD) simulations, the purposes for improvement of the curing process in the autoclave chamber are being done. CFD simulations are able to analysis the fluid flow in a certain space with several parameters like velocity, density, pressure, temperature, and viscosity. To analysis the aeroplane wing in the autoclave curing chamber, the represented model is put inside the chamber and analysis through CFD.

In this research, the objectives of the autoclave have to fulfill a requirement of the model of an aeroplane wing size about 2m weight, 1m height, and 5mm thickness. Therefore, the design of the autoclave chamber dimensions must be wider than the aeroplane wing's dimensions with 13m length and 3m of radius cylindrical shape chamber.

Nowadays simulation has used as a prediction for most of the specialized categories not only included for the industry. Simulation acts as a second chance to avoid any mistakes that happened before the actual test-drive experiment that cost expensively. The problems of the curing process for aeroplane wings need a huge concrete chamber that cost significantly. Thus, the simulation is the best choice to estimate the dimensions and other related properties of the chamber before the real construction of it.

The autoclave chamber has several scales for different type production purpose such as range of 12 inches diameter X 24 inches length for small scale production, 60 inches diameter X 240 inches length for medium scale production inches and 120 inches diameter X 240 inches length for large scale production. These standard models type autoclaves are normally used for composite curing autoclave technology. There is custom-made autoclave with for another process that includes wood, glass, dewaxing, and AAC concrete. Normally, the chamber is made up of stainless steel with the cylindrical shape-like tube.



1.1 PROBLEM STATEMENT

Nowadays, air transportation used for crossing from one country to another. The process of improvement and sub-parts of airplane has to be fast produced and easy to change for commercialized purposed. Therefore, the new autoclave chamber has to be designated for the curing process of the composite parts. To achieve fast curing process for an aeroplane wing, the inlet air flow velocity and temperature distribution in the chamber should be controlled to cure the composite at the specified condition. When the heat distribution in the chamber is not uniform, the flow of fluid inside the chamber will not flow smoothly throughout the whole chamber but will form vortexes along the path of flow. At the center of circulate flow, the stagnation area appeared and it caused the velocity approximate to zero. Therefore, the elimination of the stagnation area should able to improve the curing efficiency inside the chamber. The efficiency of the autoclave is based on reduction of cycle time. Reduction of cycle time basically based on both the temperature uniformity of airflow and achieving uniformity in the velocity of the airflow inside the chamber in this project.

UNIVERSITI TEKNIKAL MALAYSIA MELAKA

1.2 OBJECTIVES

- To investigate the velocity and temperature distribution inside an autoclave
- To determine the suitability of exhaust fan or pressure outlet at outlet boundary condition for uniform temperature distribution
- To determine the stagnation area inside the autoclave

1.3 SCOPE

The research project will be priority focus on the controllable variables that not customized such as the fan size with radius of 1m, inlet size dimension of air flow (nozzle), model size dimension of 2m X 1.6m X 5mm, inlet air velocity in range of 1 to 5 m/s and the chamber dimension about 4.5m X 4.5m X 4.0m. Moreover, the temperature inside the chamber has to be fixed accordingly due to the material of the chamber to avoid any additional heat lost to the surrounding. Other aspects such as detailed pressure distribution, the detail function of autoclave and improvements on design are not covered in this project.

CHAPTER 2

LITERATURE REVIEW

2.1 THE CONCEPT OF OVENS AND AUTOCLAVES

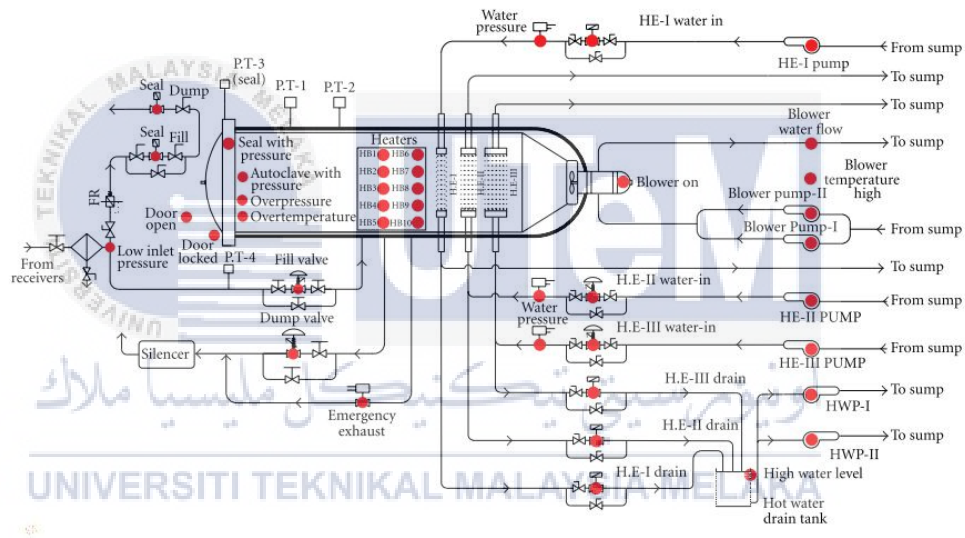


Figure 2.1: The mimic of autoclave systems (Ramaswamy Setty *et al.*, 2011)

Basically, autoclave consists of several main systems that contain certain parts of autoclave machine. The main part of the system is the pressurized system which correlated towards the heating system. The pressurized system which contains the main shell and quick-lock door to create a completely sealed space for sterilization where the temperature increases together with pressure inside the main shell. The heating system is built up from some heating coils which attached on the inner wall of the main shell. The heating system provided indicates

the result of one megawatt of heater capacity is needed for an autoclave with a size of diameter about 4.5m and length of 9m. To maintain the uniformity of the air flow inside the autoclave, the air circulation system is provided with aids of the blower fan. There is a cooling system inside the autoclave not simply to reusing the condensed water while for another extra process like cooling progress and icing process. (Ramaswamy Setty *et al.*, 2011) Furthermore, the pressurization system of the autoclave is using a rate of 2 bar/min with the inlet gas of nitrogen as the medium instead of air. Due to air is far more inflammable inside autoclave which in the end cause massive loss towards the sterilized instruments, therefore the nitrogen gases able to ensure the autoclave cure cycles run in a fire-free condition. Figure 2.1 is a mimic of the autoclave.

Furthermore, due to the large scale of actual refers autoclave, the used autoclave is on a smaller scale with a certain ratio compared to the actual. Therefore, a validation by using the previous model is made through simulating the same dimension of autoclave model. The validation is purposely to indicate the feasibility of the simulation on that particular case and to determine the result of the made simulation with the references to have a comparison. Figure 2.2 is the view of the sample of the model used for validation, it consists of a cylinder act as autoclave with a size of 2000mm×4000 mm, with a large frame mold with the size of 3200mm×1600mm×850 mm. (Xu *et al.*, 2017)

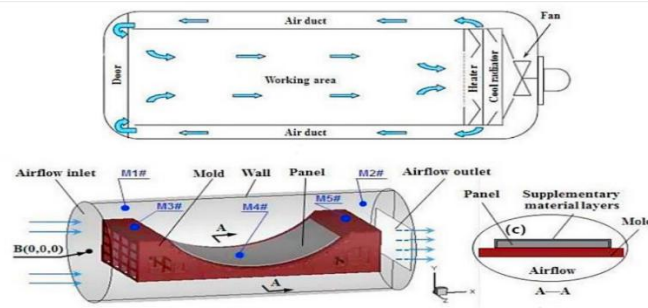


Figure 2.2: The model of the sample used for validation purpose (Xu *et al.*, 2017)

Autoclave also capable in curing of composite material which strengthening the material through the reposition of inner particles under high temperature. The phenomenon that causes the exposing metal under a high-temperature environment to achieve the enhancement of metal is called stress relaxation. (Holman, 1989) With the assists of thermal stress relaxation, the contour of the metal specimen remains and the inner fiber of metal is protected from the stress beyond their yield stress. It is used to retain all of the properties of a metal specimen while changing its shape. The slightly changing of shape after curing process is due to the elasticity of the inner metal fiber. It has said that the autoclave is suited to be used for forming panels for the aircraft and aerospace structures. Figure 2.3 shows the curing process of the specimen.

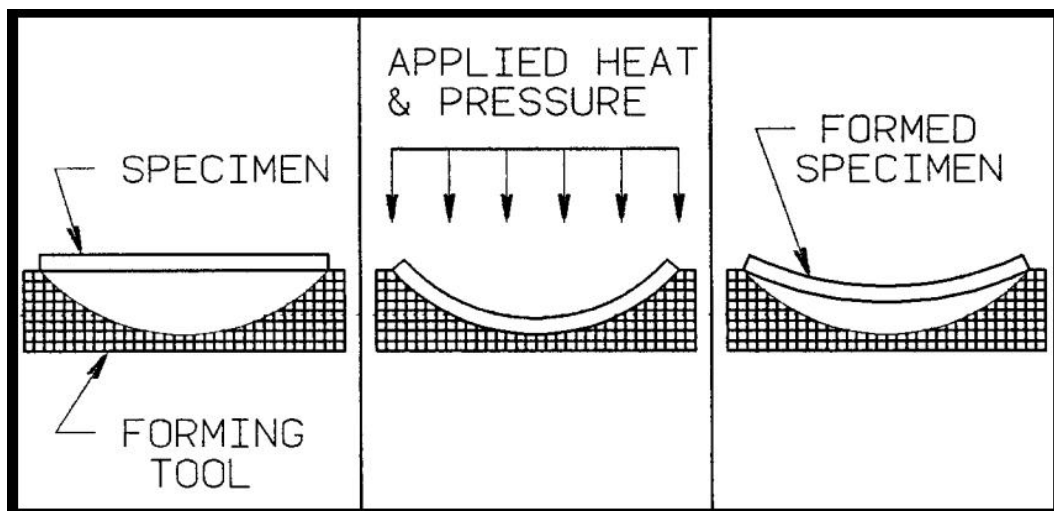


Figure 2.3: The curing process for metal specimen inside the autoclave (Holman, 1989)

Basically, the oven is considered as a machine for heating up things to achieve different purpose like microwaving the food. Figure 2.4 shows the main element of oven included five walls (bottom, right, left, rear and top), glass door and the air cavity. (Lucchi and Lorenzini, 2019)

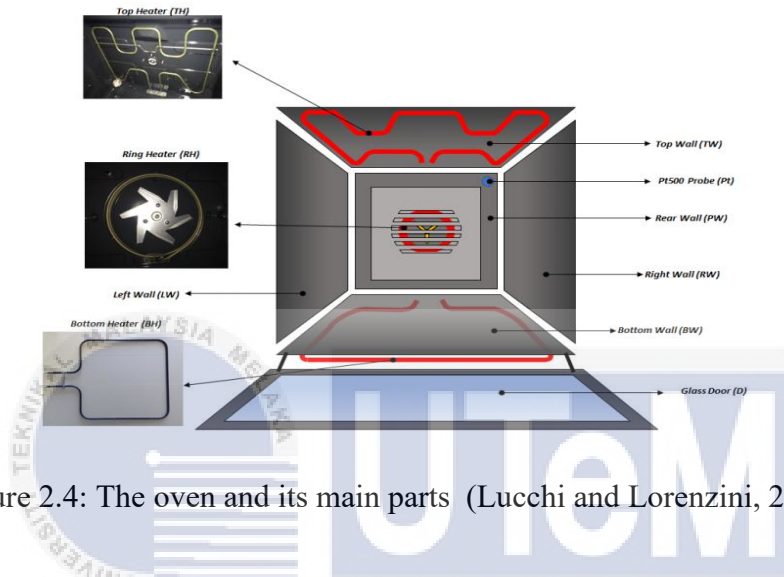


Figure 2.4: The oven and its main parts (Lucchi and Lorenzini, 2019)

The study of the oven is made to understand the specific setting inside the oven which related to its result. (Burlon *et al.*, 2017) By studying the research on the oven, the heat flow inside is able to comprehend clearly. Figure 2.5 is an example of the oven to study the evaluation of energy performance during both steady state and transient state operation.

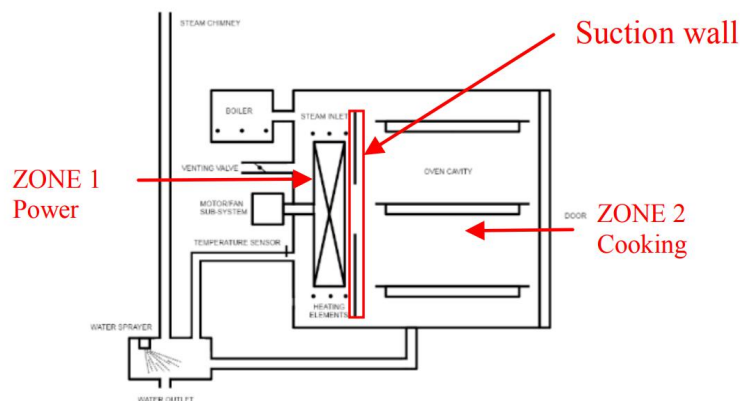


Figure 2.5: The cross diagram of the oven and its particular usage (Burlon *et al.*, 2017)

2.2 FLOW VISUALIZATION OF OVENS AND AUTOCLAVES

Furthermore, to investigate the inlet position and size of the air flow that will trigger the temperature distribution inside the autoclave chamber changes, the particular journal that research on the method and way for the inlet air flow is studied. (Park *et al.*, 2018) It has shown that different location for the inlet can cause air vortex occurring that lead to another problem that air velocity at vortexes is approximately zero thus affect the heat transfer for the curing process. Figure 2.6 is the inlet air flow patterns for 3 significant case.

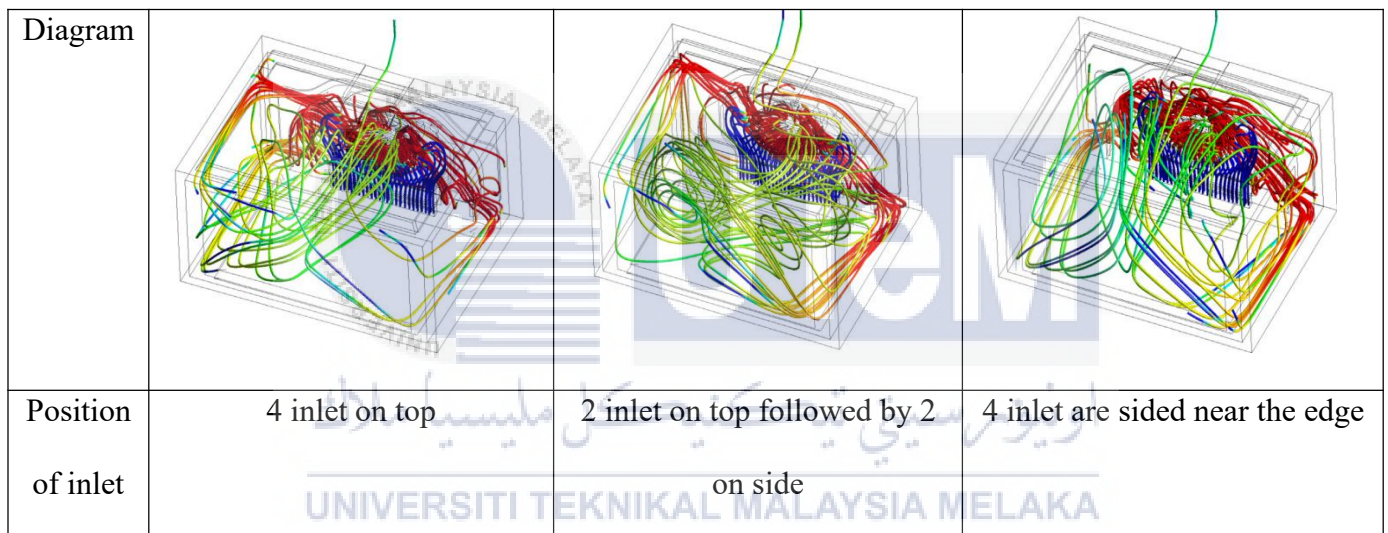


Figure 2.6: Figure of different inlet against the heat flow pattern (Park *et al.*, 2018)

To control the inlet air flow velocity, aids of heater and nozzle at a different location is studied to maximize the efficiency of heat flow for the curing process. As the reason for lacking research raw materials, soldering reflow oven operation type journals are used for references to control the uniform distribution of heat inside the whole autoclave chamber. (Illés and Bakó, 2014) Figure 2.7 has clearly shown that the heat distribution of the inlet air flow is controlled through the aids of several nozzles to achieve uniform temperature throughout the whole process.

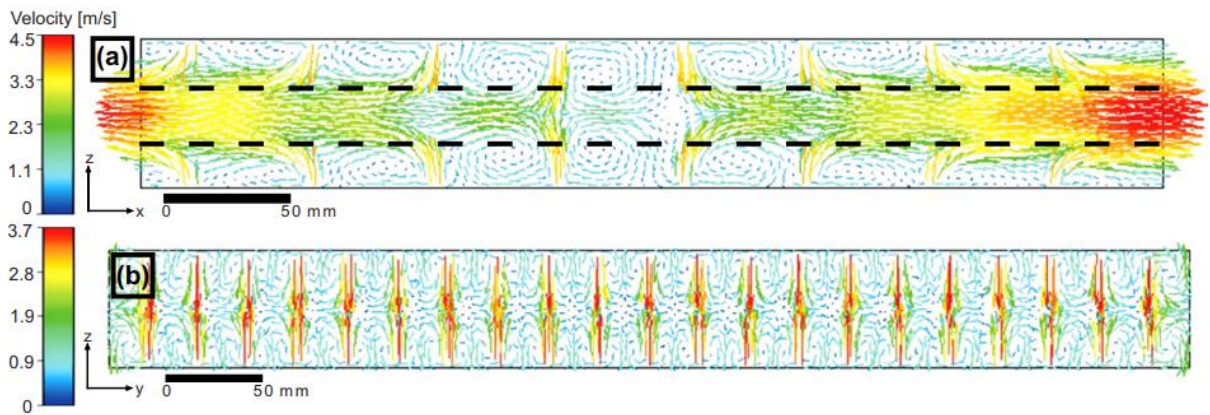


Figure 2.7: The air velocity flow diagram with temperature differences (Illés and Bakó, 2014)

When the conveyor belt moving along the whole soldering oven, with the different load is placed on a different location to further study about the airflow when there is an obstacle along with it. Figure 2.8 has shown the air flow when some loads placed on a different location on the conveyor belt:

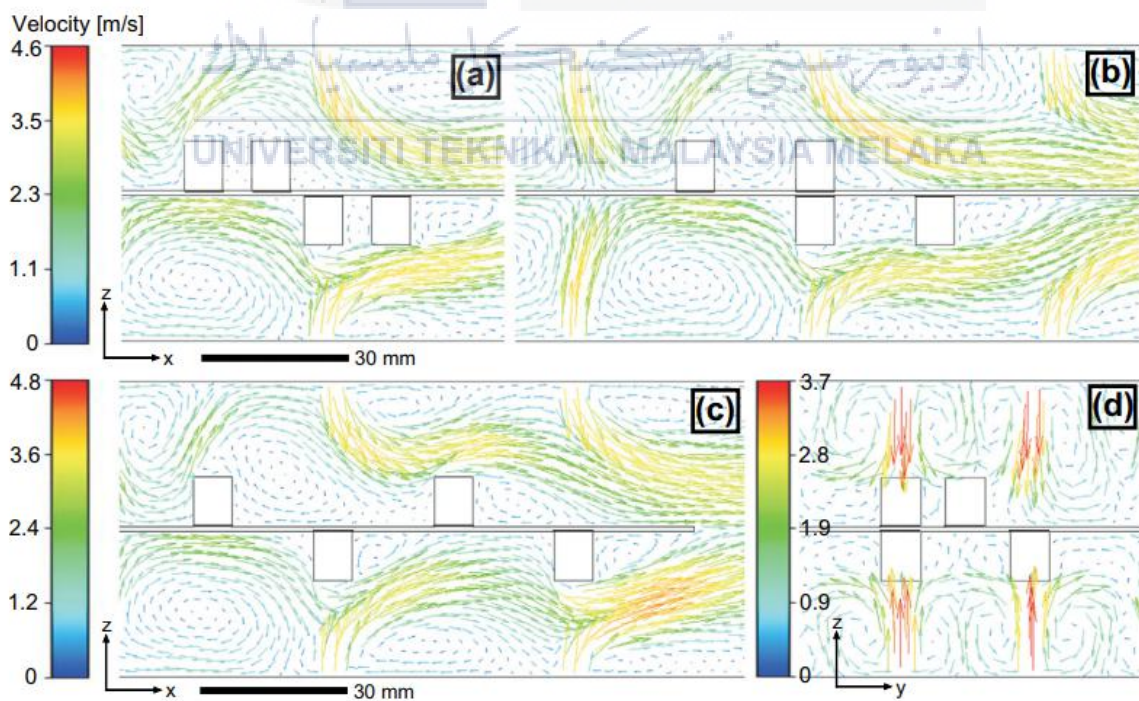


Figure 2.8: The flow pattern inside the oven when obstacles are placed (Illés and Bakó, 2014)

From Figure 2.8, it has clearly shown that vortexes are forming on certain places due to the non-uniform flow and the velocity around the obstacles are slowed down. From d, it has clearly shown the vortexes formed between two fixed inlets.

The study of heating and air circulating system inside the autoclave is the essential research to improve the function of autoclave through several additional functions. The basic schematic diagram of an autoclave's air circulation and heating system are shown in Figure 2.9. (Ramaswamy Setty *et al.*, 2011)

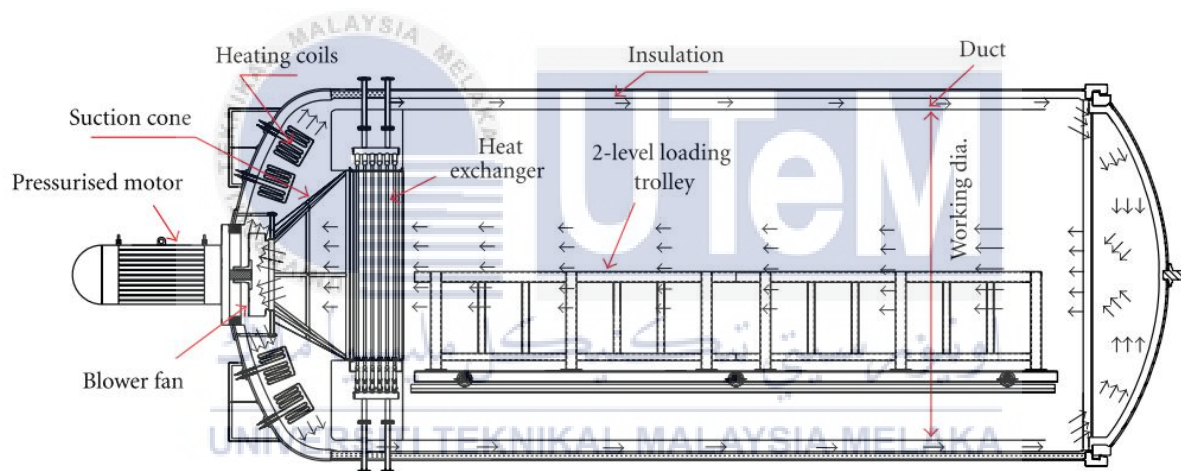


Figure 2.9: The schematic diagram of air circulation inside an autoclave (Ramaswamy Setty *et al.*, 2011)

The study on the inner air circulation of the oven is to apply the idea of the oven on the autoclave since both of them are using heat transfer to achieve a certain purpose in an occupied space. Figure 2.10 has shown that the heat flow through the whole coke oven. (Burlon *et al.*, 2017) The inlets of heated air are placed on the top of the oven and it shows the heat flow down through all the oven. The downwards hot air is the medium that complete the coking process.

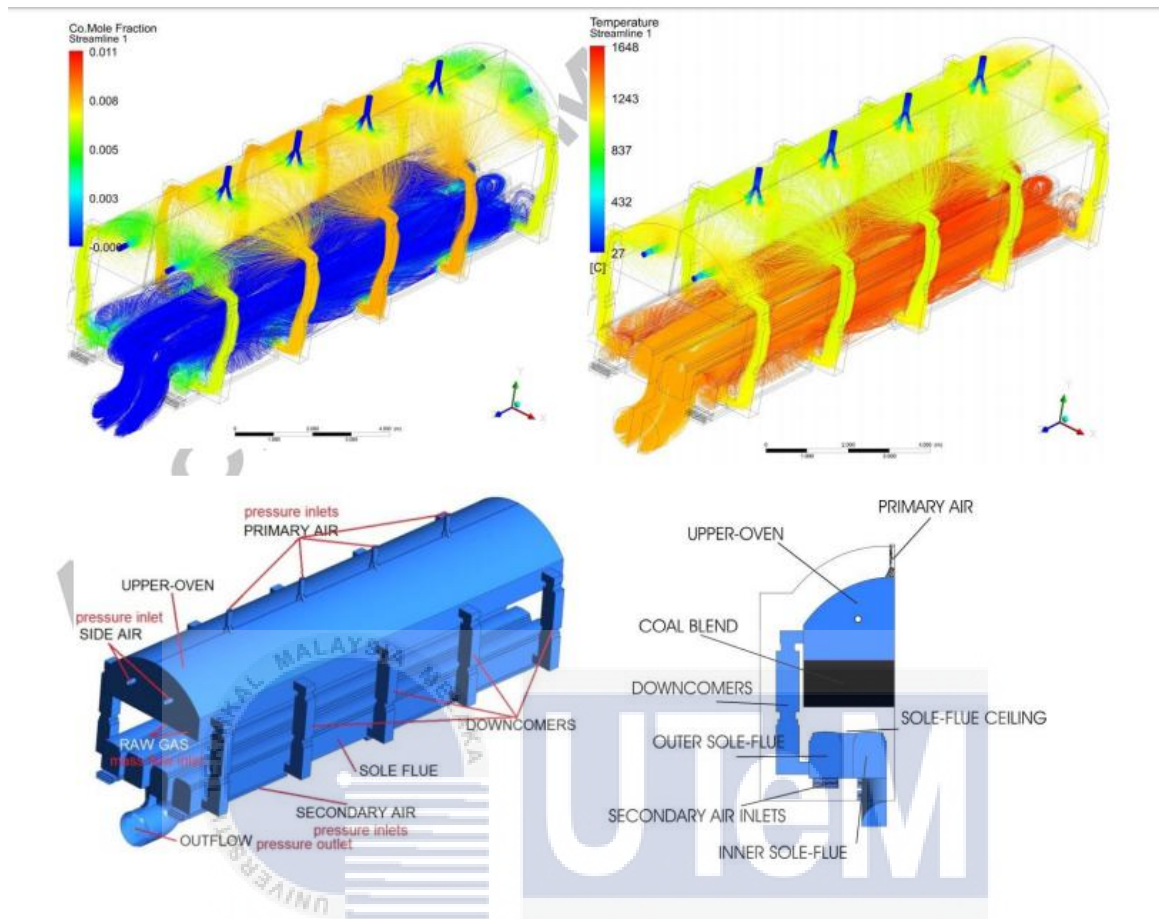


Figure 2.10: The heated air flow of a coke oven with its structure (Burlon et al., 2017)

Moreover, from the cross diagram of the heat flow of the coke oven, it has clearly shown that the heated air is flowing downwards from both left and right inlets and the meeting of heated air from both sides have formed a circulating cortex which can trap the heat. The vortexes also considered as a stagnation point that all the heat is compressed towards the point and causes the stagnation point has a higher temperature than other location. The cross diagram of the coke oven with heat flow is shown in Figure 2.11.

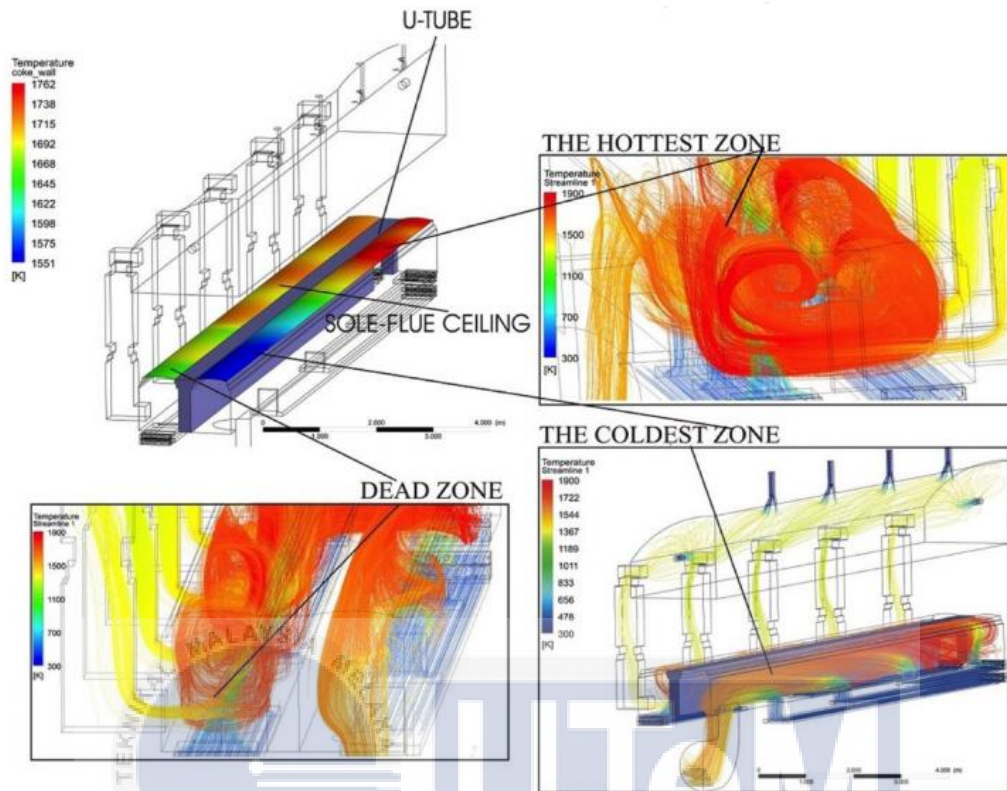


Figure 2.11: The overview of heat flow across the coke oven (Burlon et al., 2017)

Streamline can be defined as a line that flow fluid along with it mostly are smooth which meant laminar flow for the majority of that fluid. From the streamline diagram, the velocity surrounding model is determined. In Figure 2.13, it shows that the velocity decreases significantly when attached to the model surface (Chen, Zhan and Xu, 2014)

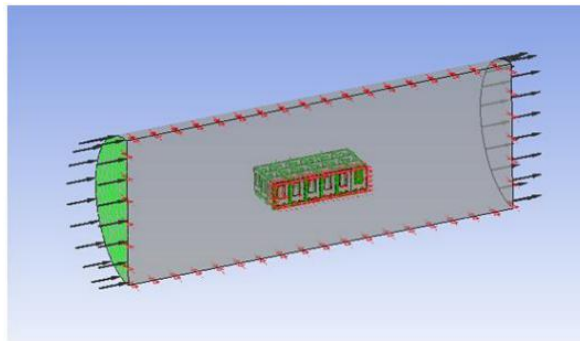


Figure 2.12: The airflow of the autoclave model (Chen, Zhan, and Xu, 2014)

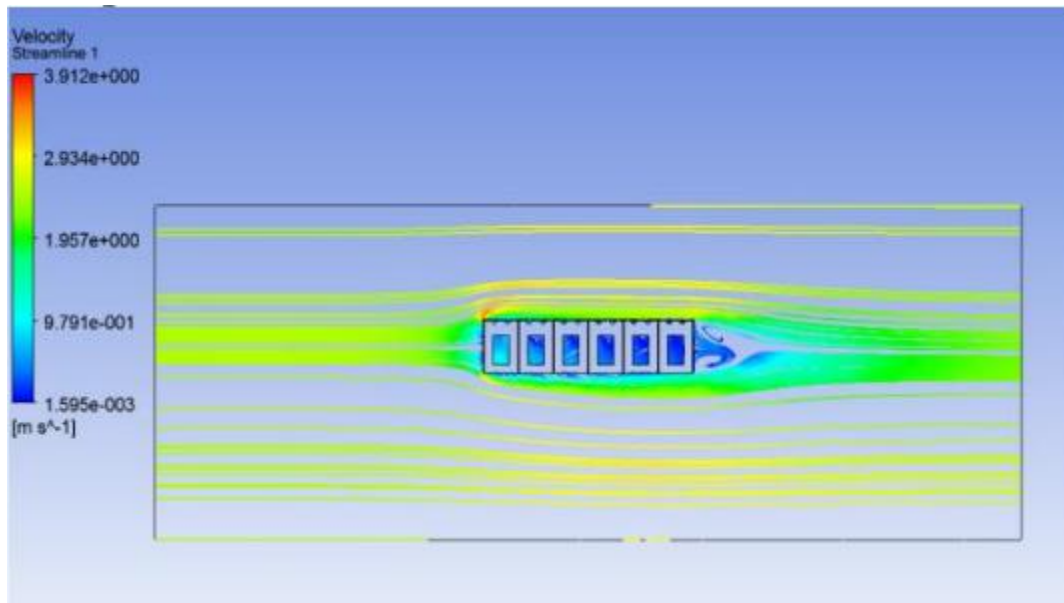


Figure 2.13: The streamline of the symmetrical plane (Chen, Zhan, and Xu, 2014)

Other than that, autoclave also used in the chemical production category. One of the examples is LDPE production. An autoclave is used in the mixing process for the production of low-density polyethylene with a stirring shaft. (Zheng et al., 2014) Figure 2.14 shows the flow inside the autoclave stirrer with a different type of impeller of the stirrer.

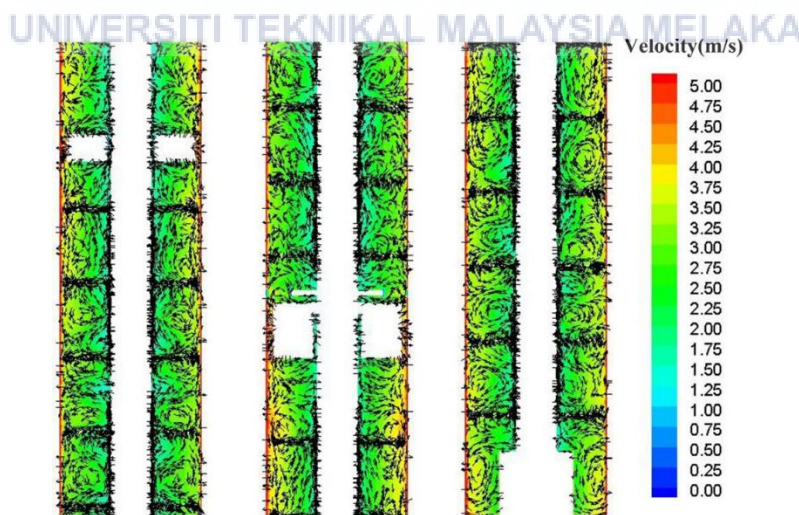


Figure 2.14: The velocity distribution of LDPE autoclave reactor with different impellers (Zheng et al., 2014)

2.3 TEMPERATURE DISTRIBUTION OF OVENS AND AUTOCLAVES

Furthermore, the temperature distribution inside the oven also affected by the blockage of air flow inside the oven. With an obstacle inside the pathway of heat flow, the pattern of heat flow is affected. The path of heat conduction is blocked by the obstacle and causes the reduction of the number of heat transfers. (Yi *et al.*, 2017) Therefore, the velocity of flow fluid is decreased approximately to zero. The nearly zero velocity of heat flow has trapped the heat and form a stagnation point inside the oven with high temperature at the center of the point.

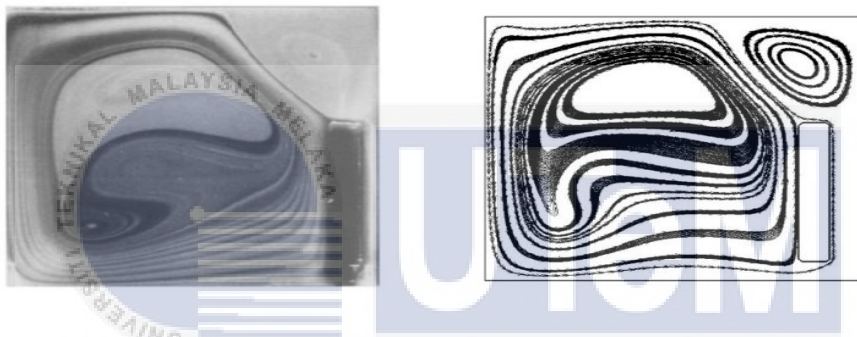


Figure 2.15: The streamline pattern and the present simulation (Yi *et al.*, 2017)

Moreover, the temperature distribution of the oven can explain by examine the items that heated inside the oven. (Kokolj, Škerget, and Ravnik, 2017) Figure 2.16 shows the temperature of the baking tray inside the center of the oven during a period of time. From Figure 2.16, the temperature field shows that the flow of heat air is a trend towards the right-side of the baking tray.

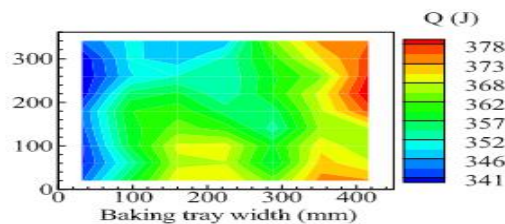


Figure 2.16: The temperature field simulation inside the oven (Kokolj, Škerget, and Ravnik, 2017)

Meanwhile, autoclave mostly used in the manufacturing of composite material. In the aircraft curing process, autoclave used to cure the fairing and other relative tools. In Figure 2.17, it shows the temperature distribution of the curing process at 60 minutes after curing starts. The temperature at the fairing is higher than surrounding and the mold's temperatures which indicate the heat among the curing process are mainly focusing on the fairing. (Zeng and Raghavan, 2010)

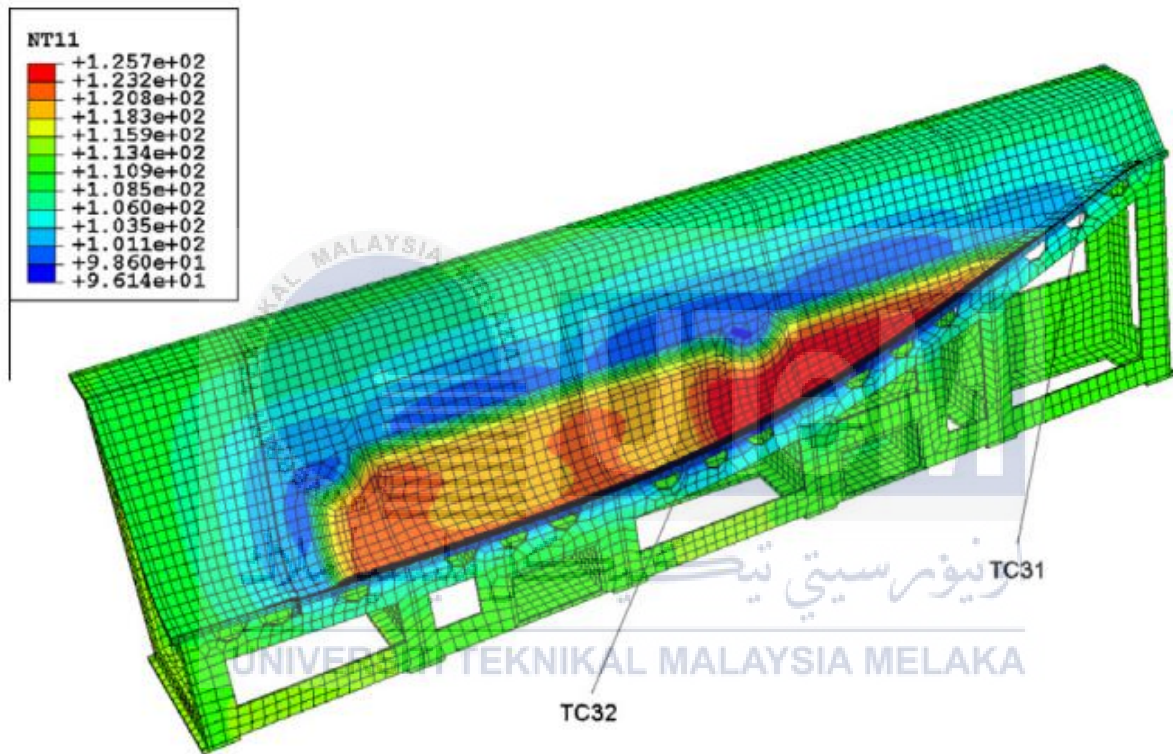


Figure 2.17: The temperature distribution of the fairing and tools at 60 minutes (Zeng and Raghavan, 2010)

With the irregular shape of the edge of used toolings, some of the heat flow inside the autoclave is reduced. This phenomenon causes some parts which located further from the inlet of heated air are in a lower temperature field compare to the parts that stay in front. (Weber *et al.*, 2016) Figure 2.18 shows the temperature distribution of a modal with the inlet of the heat source.

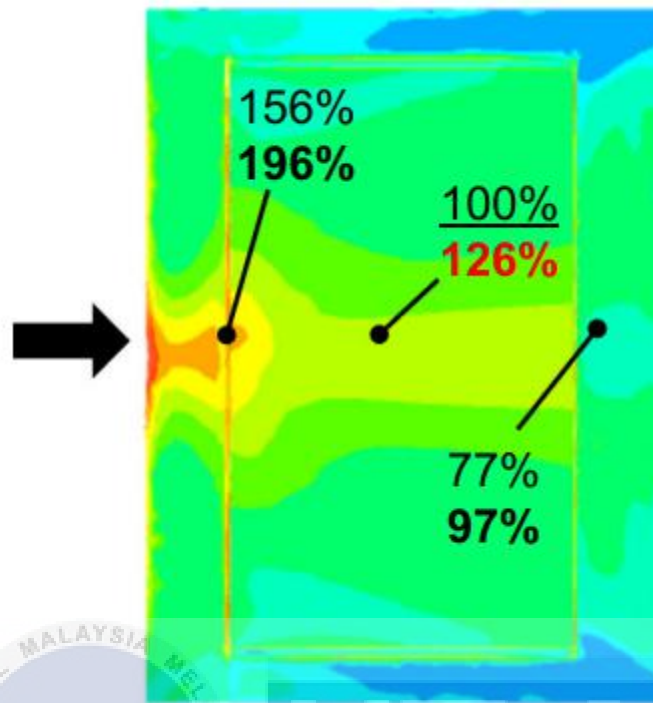


Figure 2.18: The temperature distribution on the surface of the model (Weber *et al.*, 2016)

2.4 CURRENT DESIGN TO OPTIMIZE THE PERFORMANCE IN BOTH OVENS AND AUTOCLAVES

Other than that, modeling the airflow inside the chamber also able to improve the curing cycle time. Through the validation of a simple modification by increasing the conveyer belt moving speed to increase the temperature velocity of air for reduction of the curing cycle time. (Yi *et al.*, 2017)

The performance of a coke oven with conveyer belt able to improve by controlling others settings inside the process. One of the method is reducing the curing cycle. Figure 2.19 and 2.20 has clearly show the graph of inner temperature of oven with distance to achieve uniform temperature. With the modification of conveyer belt moving speed, the temperature distribution inside the oven able to reach a uniform temperature state. Figure 2.21 shows the conclusion of different modification affect towards the curing cycle time.

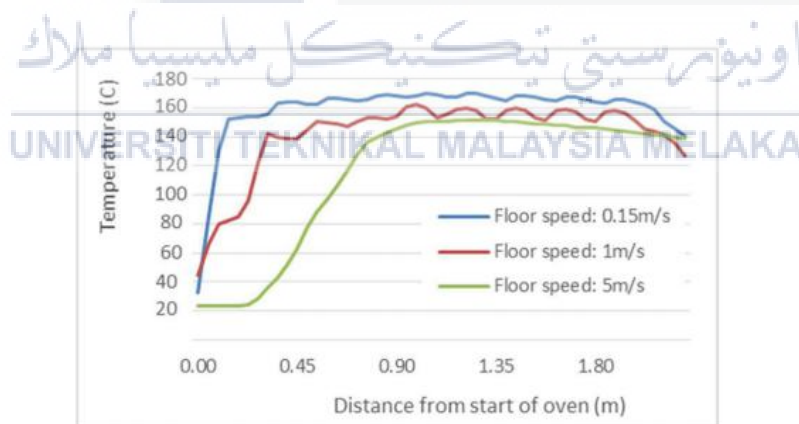


Figure 2.19: The references for conveyer belt speed (Yi *et al.*, 2017)

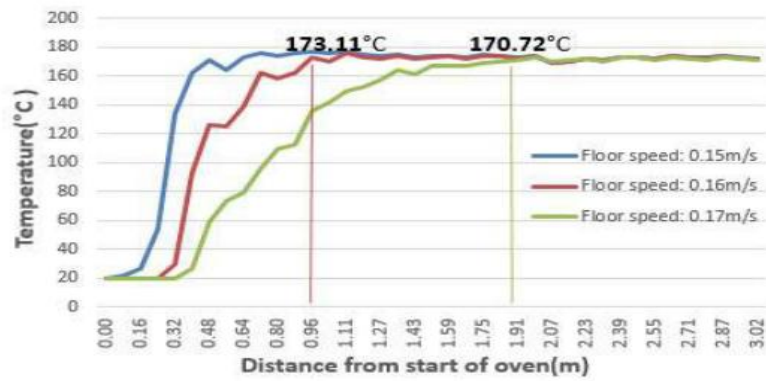


Figure 2.20: The modified conveyer belt speed (Yi *et al.*, 2017)

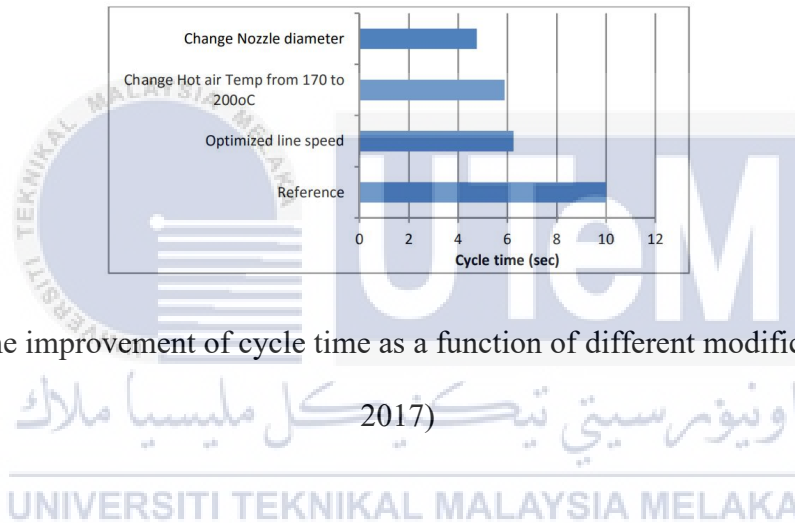


Figure 2.21: The improvement of cycle time as a function of different modification (Yi *et al.*, 2017)

CHAPTER 3

METHODOLOGY

The general methodology used throughout this project shown in Figure 3.1.

The numerical works was used to obtain the result and related data. It included the design of the model domain for the aeroplane wing with dimension 2.0m X 1.6m X 5.0mm. It followed by the meshing process with a different type of meshing such as 2-dimensional and 3-dimensional to maximize efficiency. After decided meshing type, material properties set-up and boundary condition set-up are placed accordingly. Re-meshing was done to ensure high quality result with a scale of smaller mesh sizes.

UNIVERSITI TEKNIKAL MALAYSIA MELAKA

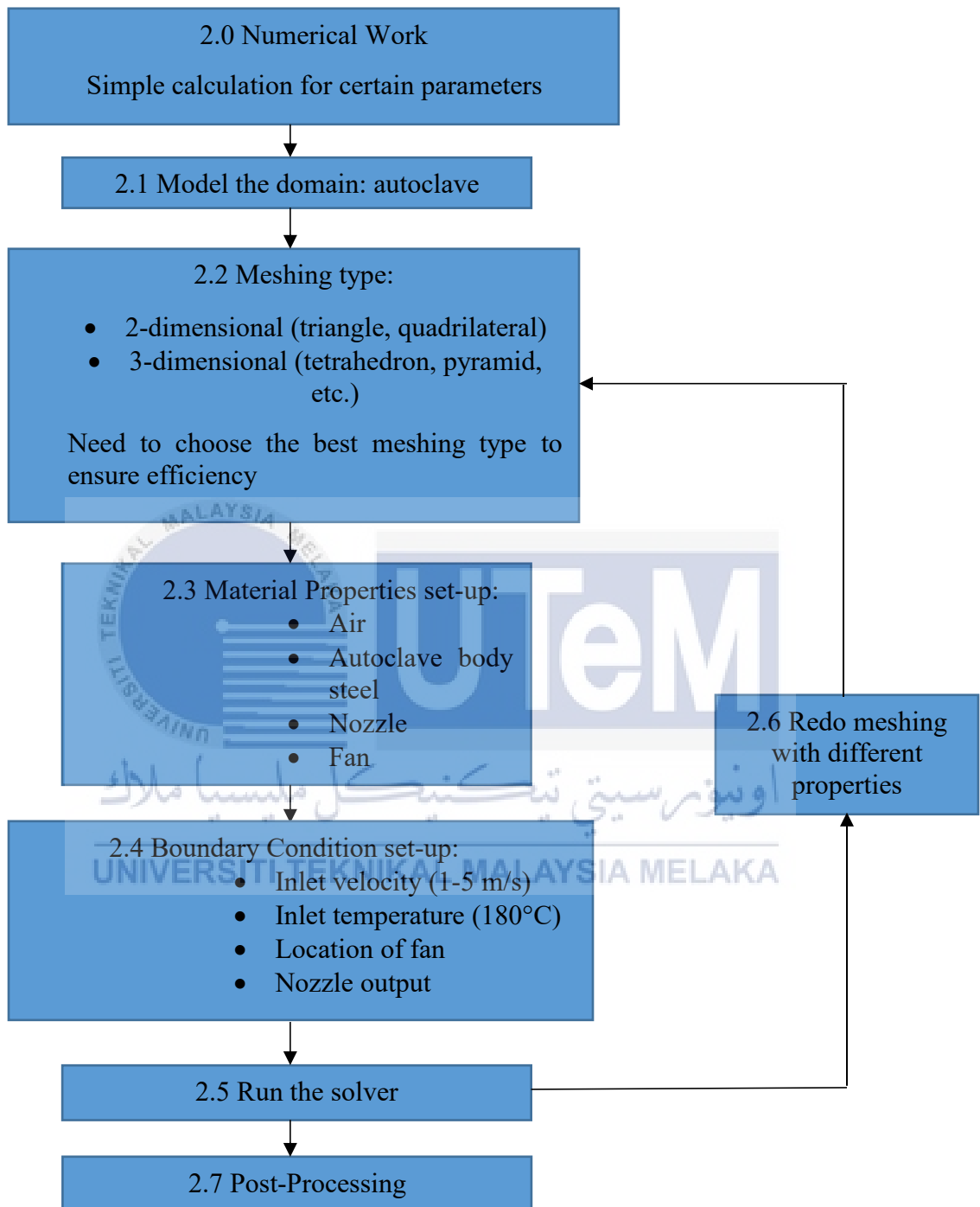


Figure 3.1: The general methodology used.

3.2.0 NUMERICAL WORK

In order to fix the inlet air flow together with the applying nozzles and fans, the conservation of mass equation is used. The conservation of mass indicates that the mass inside a specific volume with the continuous inlet and outlet remains as the amount of mass regardless of its shape, density, and volume. Therefore, the mass flow rate of the specific volume is constant. The equation of conservation of mass is shown below:

$$mass\ flow_{in} = mass\ flow_{out} \quad (3.1)$$

$$Area\ of\ cross\ section_{inlet} \times velocity_{inlet} = Area\ of\ cross\ section_{outlet} \times velocity_{outlet}$$

If nozzles are added up into the autoclave chamber, the inlet of air through the nozzle is calculated by comparing both mass flow rate of nozzle and autoclave chamber. By assuming the dimension of nozzles used as a cylinder with a radius of 100mm and applying the dimension of validation sample above,

$$A_{nozzle} \times velocity_{nozzle} = A_{chamber} \times velocity_{chamber}$$

Other than that, Navier-stoke equation is included in the FLUENT app to determine the velocity distribution of flow inside a fluid with some initial condition applied. Following are the equations that used inside the FLUENT :

$$\text{General Continuity Equation: } \frac{\partial \rho}{\partial t} + \frac{\partial(\rho u)}{\partial x} + \frac{\partial(\rho v)}{\partial y} + \frac{\partial(\rho w)}{\partial z} = 0 \quad (3.2)$$

Other than that, the motion is combined through 3 axes which are X-axis, Y-axis, and Z-axis. Following are the equation of motion for 3 axes momentum, where u, v, w are represent the axis-velocity of X-axis, Y-axis, and Z-axis accordingly.

Equation of Motion:

$$\text{X-Momentum: } \frac{\partial(\rho u)}{\partial t} + \frac{\partial(\rho u^2)}{\partial x} + \frac{\partial(\rho uv)}{\partial y} + \frac{\partial(\rho uw)}{\partial z} = -\frac{\partial p}{\partial x} + \frac{1}{Re_f} \left[\frac{\partial \tau_{xx}}{\partial x} + \frac{\partial \tau_{xy}}{\partial y} + \frac{\partial \tau_{xz}}{\partial z} \right] \quad (3.3)$$

$$\text{Y-Momentum: } \frac{\partial(\rho v)}{\partial t} + \frac{\partial(\rho uv)}{\partial x} + \frac{\partial(\rho v^2)}{\partial y} + \frac{\partial(\rho vw)}{\partial z} = -\frac{\partial p}{\partial y} + \frac{1}{Re_f} \left[\frac{\partial \tau_{xy}}{\partial x} + \frac{\partial \tau_{yy}}{\partial y} + \frac{\partial \tau_{yz}}{\partial z} \right] \quad (3.4)$$

$$\text{Z-Momentum: } \frac{\partial(\rho w)}{\partial t} + \frac{\partial(\rho uw)}{\partial x} + \frac{\partial(\rho vw)}{\partial y} + \frac{\partial(\rho w^2)}{\partial z} = -\frac{\partial p}{\partial z} + \frac{1}{Re_f} \left[\frac{\partial \tau_{xz}}{\partial x} + \frac{\partial \tau_{yz}}{\partial y} + \frac{\partial \tau_{zz}}{\partial z} \right] \quad (3.5)$$

Where u is the velocity in X-axis, v is the velocity in Y-axis, and

w is the velocity in Z-axis.

Basic Reynolds Number Equation also used in determining the type of flow of fluid. This is used to insert the type of flow into the setting of boundary condition during CFD simulation.

$$\text{Reynolds Number Equation: } Re = \frac{\rho u L}{\mu} = \frac{u L}{\nu} \quad (3.6)$$

To perform a turbulence flow that all the vortexes of the flowing fluid are under control, the concept on the vorticity of fluid is needed. In a simple way, vorticity is a whirling pattern of fluid which similar to angular momentum in solid, where normally the vorticity is in a form of vectors.

$$\text{Vorticity vector, } \omega = \nabla \times v = \left(\frac{\partial v}{\partial z} - \frac{\partial w}{\partial y} \right) i + \left(\frac{\partial w}{\partial x} - \frac{\partial u}{\partial z} \right) j + \left(\frac{\partial v}{\partial x} - \frac{\partial u}{\partial y} \right) k \quad (3.7)$$

From the vorticity vector in equation 3.7, it shows that the influence of vorticity is based on the velocity vector components in x, y, and z directions that represented by i,j,k.

3.2.1 MODEL THE DOMAIN

Figure 3. 2 shows the model of cylinder and brick.

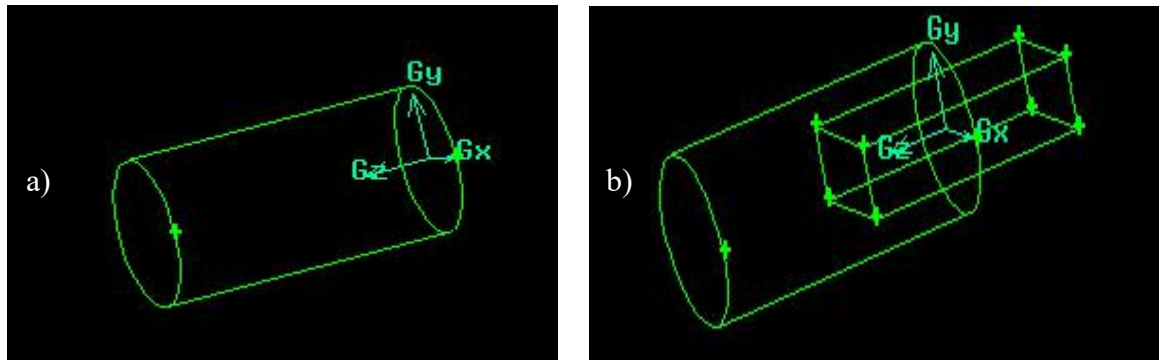


Figure 3.2: a) cylinder-like autoclave model b) combined the model with brick-shape mold

Using command of move volume, the brick-shape mold is positioned at the center of the cylinder as Figure 3.3 shown.

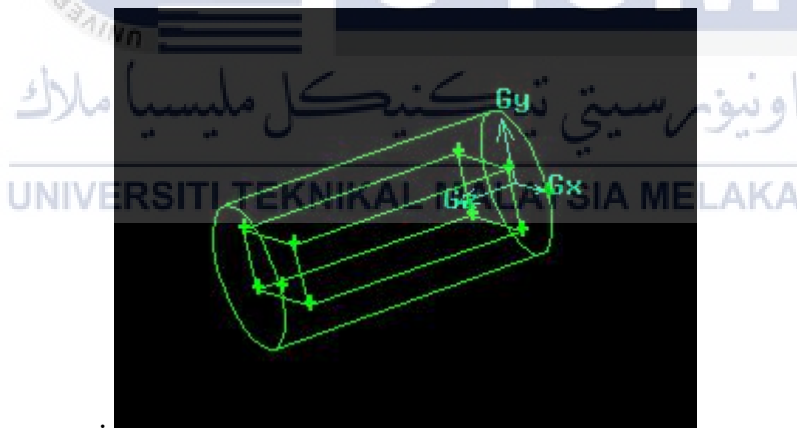


Figure 3.3: The brick is moved into the center of the cylinder

The dimension of mold is further modified by using subtract command to fix to specified shape as shown in Figure 3.4 .

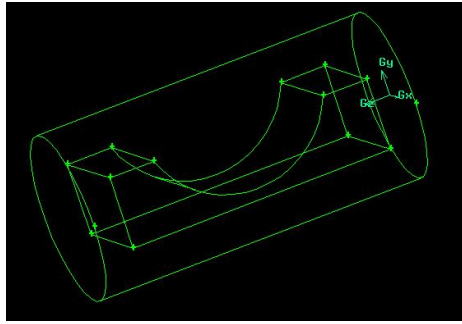


Figure 3.4: The final pattern of the sample inside gambit drawing

3.2.2 MESHING TYPE

To have a more accurate simulation result, the meshing type applied to the model is the triangle style to have a better result outcome. Using the triangle meshing, the skewness of meshing can be reduced when using square type meshing on a curved surface such as the wall of the cylinder and the curved face of the model.

Firstly, using edge meshing to adjust the gap between the marked mesh dots as shown in Figure 3.5.

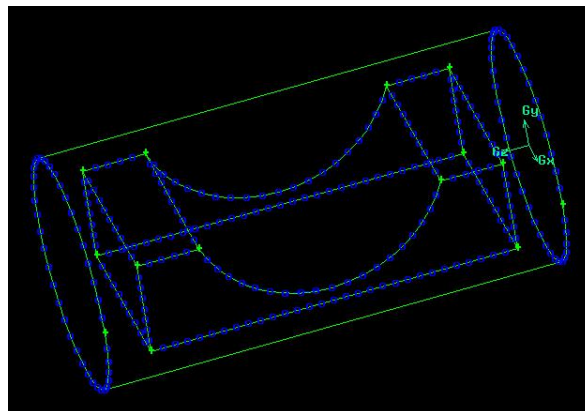


Figure 3.5: The edge meshing of sample

Continue with face meshing and volume meshing then examine the combined pattern of meshing through examine command as shown in Figure 3.6. Furthermore, the repeating of the meshing process in Gambit app is needed if any dissatisfaction occurred during simulation in FLUENT.

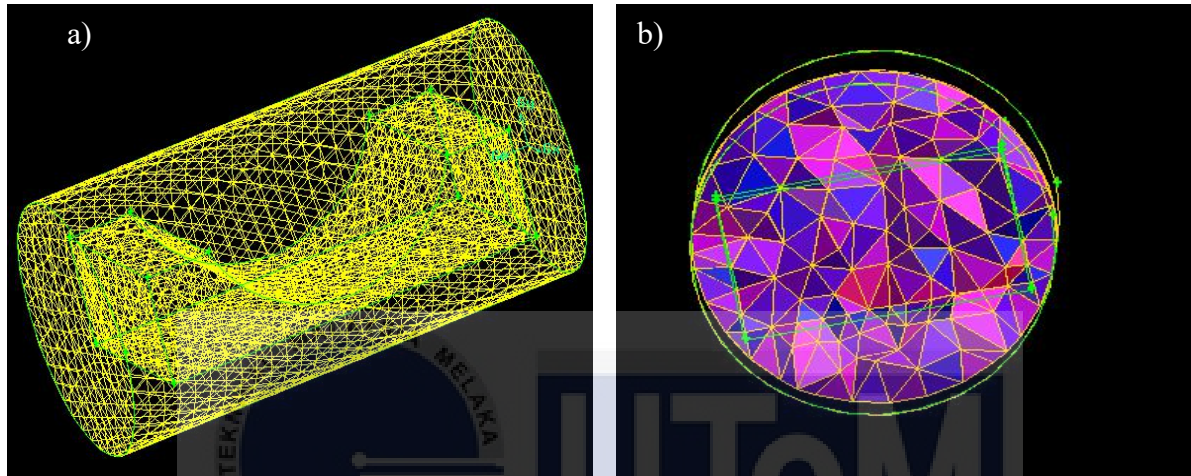


Figure 3.6: a) The final meshing b) The examined cross-section plane skewness

3.2.3 MATERIAL PROPERTIES SET-UP

The material used is mainly focused on the mold made by aluminum and the working fluid which is air. Figure 3.7 shows the properties of materials selections inside the FLUENT app.

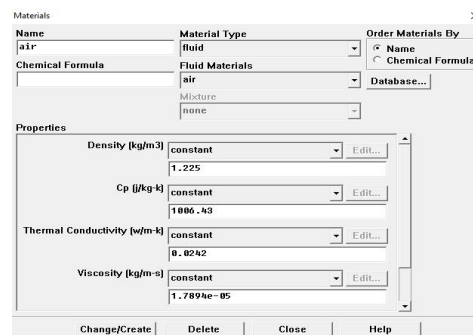
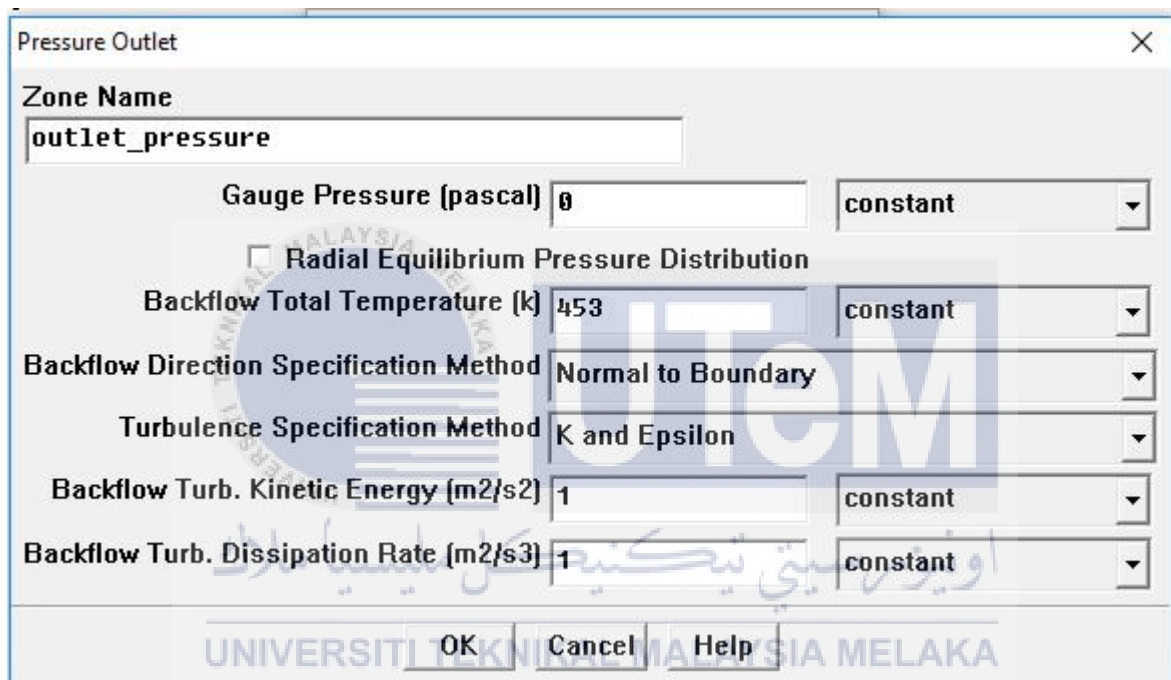


Figure 3.7: The material selection command to insert corresponding material

3.2.4 BOUNDARY CONDITION SET-UP

Besides, the boundary condition about the flowing fluid has to be set through the FLUENT app. With the command of Boundary condition inside the Define choice in FLUENT, the insert of the value of the needed variable is made, such as inlet air velocity, temperature, and the outlet pressure. Figure 3.8 shows the way to insert value accordingly to variables.



The screenshot shows the 'Pressure Outlet' dialog box in ANSYS FLUENT. The 'Zone Name' is 'outlet_pressure'. The 'Gauge Pressure (pascal)' is set to 0, with a dropdown menu set to 'constant'. The 'Radial Equilibrium Pressure Distribution' checkbox is unchecked. The 'Backflow Total Temperature (k)' is 453, with a dropdown menu set to 'constant'. The 'Backflow Direction Specification Method' is 'Normal to Boundary'. The 'Turbulence Specification Method' is 'K and Epsilon'. The 'Backflow Turb. Kinetic Energy (m2/s2)' is 1, with a dropdown menu set to 'constant'. The 'Backflow Turb. Dissipation Rate (m2/s3)' is 1, with a dropdown menu set to 'constant'. At the bottom are 'OK', 'Cancel', and 'Help' buttons. A large 'UTEM' watermark is visible across the center of the dialog box.

Figure 3.8: The setting of pressure outlet in Boundary Condition command

3.2.5 RUN THE SOLVER

After all the settings are placed in position, run the FLUENT solver through iteration command as shown in Figure 3.9. Then, Figure 3.10 shows the way to insert the number of times of iteration for application of simulation.

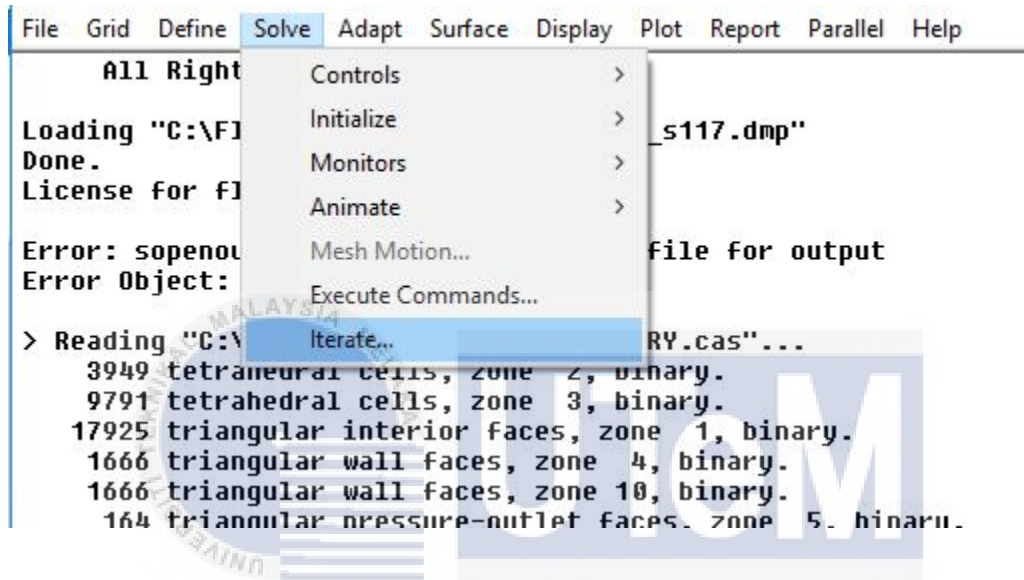


Figure 3.9: The iterate command in the FLUENT command

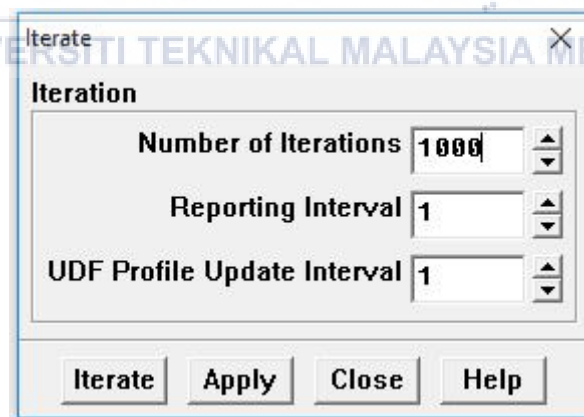


Figure 3.10: The number of iterations

3.2.6 REDO MESHING WITH DIFFERENT PROPERTIES

Repeat the process from step 3.2.0 until 3.2.5 if all the result is dissatisfied.

CHAPTER 4

RESULT & DISCUSSION

4.1 VALIDATION TOWARDS JOURNAL

Figure 4.1 shows the cross diagram of the turbulent kinetic energy of the steady-state flow in conditions of 3m/s, 1°C/min, and 0.1MPa. Figure 4.2 shows the simulated result of the project with the same condition.

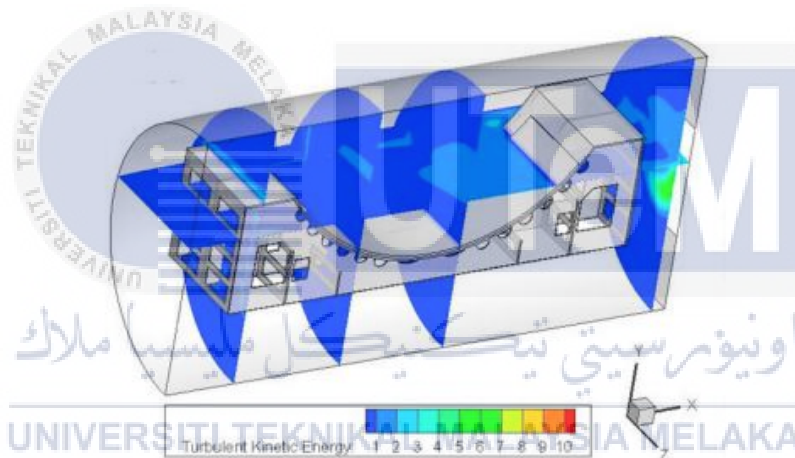


Figure 4.1: Turbulent kinetic energy of the steady-state flow of the reference (Xu *et al.*, 2017)

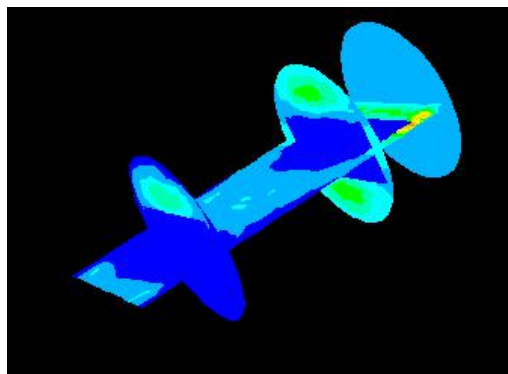


Figure 4.2: Turbulent kinetic energy of the steady-state flow of the model

It can be said that due to the different design of the model causing the slight difference between both Figure 4.1 and Figure 4.2. From Figure 3.4, it can be clearly shown that the model inside the autoclave simulation is considered as a full solid mold. But if compared clearly to Figure 4.3, the mold inside is specially designated for the improvement of air flow. The holes create spaces for the air to flow through instead of blocking. These holes are also able to minimize the velocity reduction caused by the boundary condition. Thus, the turbulent kinetic energy distribution from both Figure 4.1 and Figure 4.2 are different.

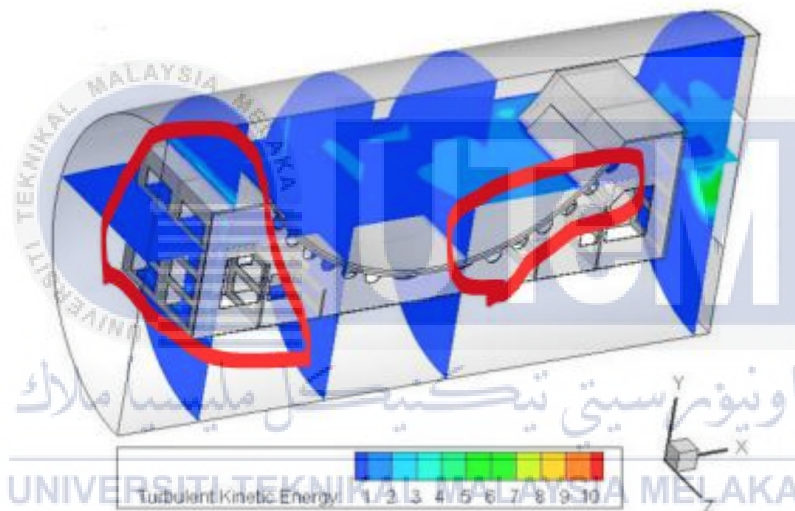


Figure 4.3: The different design of the model (Xu *et al.*, 2017)

While the efficiency of the autoclave is based on what type of autoclave and the process that involved in the autoclave. Generally, the efficiency for all type of autoclave depends on the running cycle time for each process.

It can be said that the flow pattern in the autoclave chamber is highly sensitive to the presence of mold and model. The design of mold should able to reduce blockage in air flow significantly by implementing a few empty spaces inside the mold to assist air flow.

4.2 VERIFICATION USING DIFFERENT NUMBER OF MESHING

From the validated result, one of the cases with conditions about 3m/s, 1°C/min, and 0.1MPa of the fluid flow inside the autoclave chamber is used as a validated result. The same condition with a larger number of meshing supposed to gain more detailed results. Figure 4.4 is the different type of meshing with a panel placed on mold as in the validated journal. These problems occur at the meshing part which connects to the 5mm thickness panel. There are several worse mesh parts that show at the connecting face from the panels' face. From Figure 4.4, the comments of volumetric meshing have come out with a warning that there are some errors on the meshing that related to skewness that is over large. While for Figure 4.5, the worse meshing element is determined and showed.

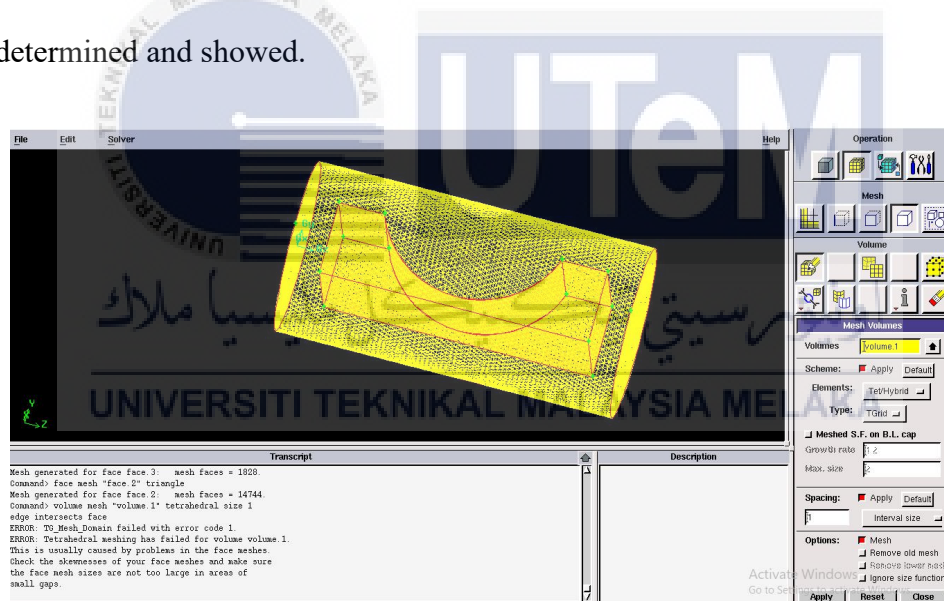


Figure 4.4: Volumetric meshing on cylindrical volume

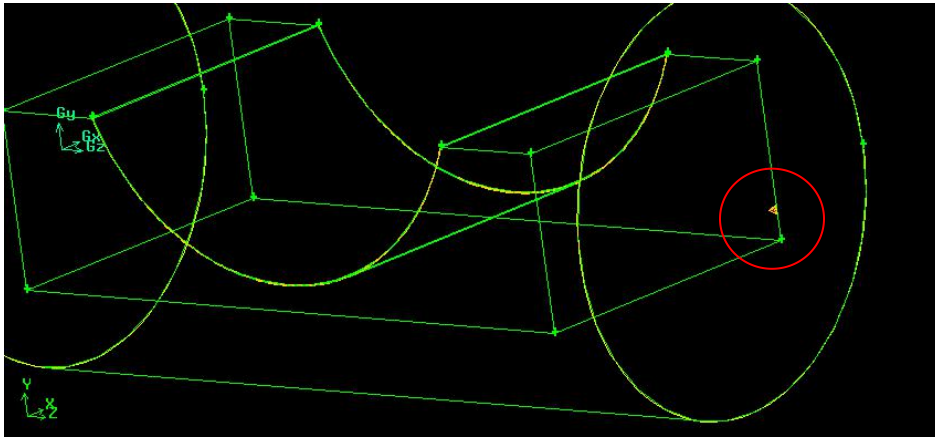


Figure 4.5: Worse meshing element occurring at aside of mold which in-contacted with cylinder volumetric mesh

Figure 4.6 shows the edges of the geometry with the represented symbol, where b is equal to g ; f is fixed; h is equal to e . Since the panel's thickness is 5 mm, therefore the geometry edges that connected with panel are set to a fixed numbers of nodes to ensure the quality of meshing for panel. For b is set to 40 nodes, f set to 3 nodes, and e with 100 nodes. Table 4.1 is the panel setting of nodes for these edges. From the Table 4.1, it has indicated that some critical edge of meshing unable to insert numbers of nodes that bigger than limited value. After remodifying some of the numbers of nodes at a cylindrical shape like channel, the meshing part still fail to mesh at volume 1 which is cylinder volume as the error and warning shown in Figure 4.7 and 4.8.

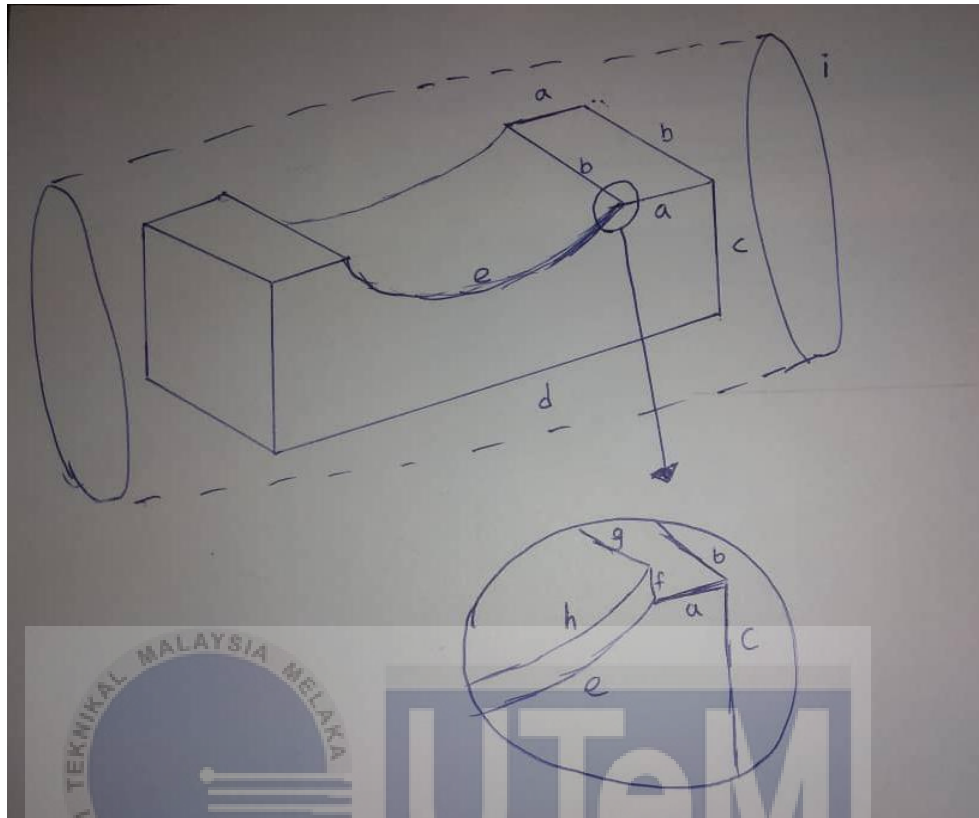


Figure 4.6: The geometry of the model with all represented edges' symbols

Table 4.1: Numbers of nodes is applied on each particular side edge

Number of the model.	Number of nodes on each side					Meshing Result
	a	b	c	d	i	
1	110	110	85	150	300	Failure on skewness
2	64	64	50	94	186	Failure on skewness
3	32	32	48	44	88	Failure on skewness

Transcript
Mesh generated for face face.3: mesh faces = 45068.
Command> face mesh "face.2" triangle
Mesh generated for face face.2: mesh faces = 365530.
Command> undo begingroup
Command> volume delete "volume.1" onlymesh
Command> volume mesh "volume.1" tetrahedral size 1
Mesh generated for volume volume.1: mesh volumes = 3064146.
Mesh of volume volume.1 contains 1308 highly skewed elements (EQUISIZE SKEW > 0.97).
Command> undo endgroup
Command:

Figure 4.7: Unaccepted meshing with skewness greater than 0.97

Transcript
Mesh generated for face face.3: mesh faces = 1828.
Command> face mesh "face.2" triangle
Mesh generated for face face.2: mesh faces = 14744.
Command> volume mesh "volume.1" tetrahedral size 1
edge intersects face
ERROR: TG Mesh Domain failed with error code 1.
ERROR: Tetrahedral meshing has failed for volume volume.1.
This is usually caused by problems in the face meshes.
Check the skewnesses of your face meshes and make sure
the face mesh sizes are not too large in areas of
small gaps.

Figure 4.8: Error showed after volumetric meshing with all the data in Table 4.1 on the cylinder

volume

Since the essential meshing part has faced a lot of problem with the additional panel on it, removing the panel simplified the meshing will improve the result. Figure 4.9 shows the model's dimensions. Table 4.2 shows 3 different models with a different number of nodes on edges.

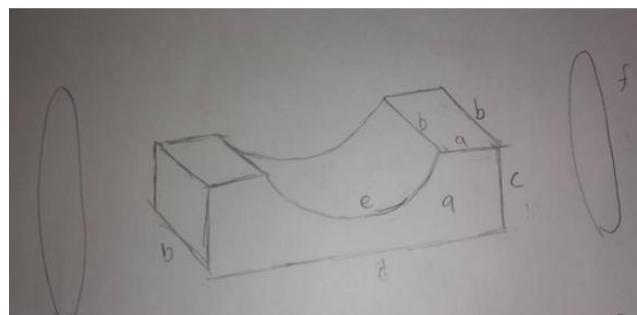


Figure 4.9: Geometry without panel

Table 4.2: Table of numbers of nodes that applied on each particular side edges for geometry without panel

Number of model.	Number of nodes on each side					
	a	b	c	d	e	f
Original (preliminary)	4	10	10	20	10	30
1	10	20	10	30	30	30
2	20	30	20	40	40	30
3	40	60	20	80	80	30

Although the validation should be made on three different meshing with all applied conditions, however, due to the long time taken for processing, therefore, the validation is specifically made on the 3rd model in Table 4.2 since it represents the larger number of meshing which indicates the results of simulation should be the most suitable.

4.3 COMPARISON ANALYSIS OF BOUNDARY CONDITION OF PRESSURE OUTLET AND EXHAUST FAN

To further analyze the effect of boundary condition towards the result of air flow inside the autoclave, the same condition of 0 pascal pressure is applied at both conditions. The table 4.3 shows the result for both simulations which air inlet flow from left to right with a condition of 3m/s at 0 pascal condition.

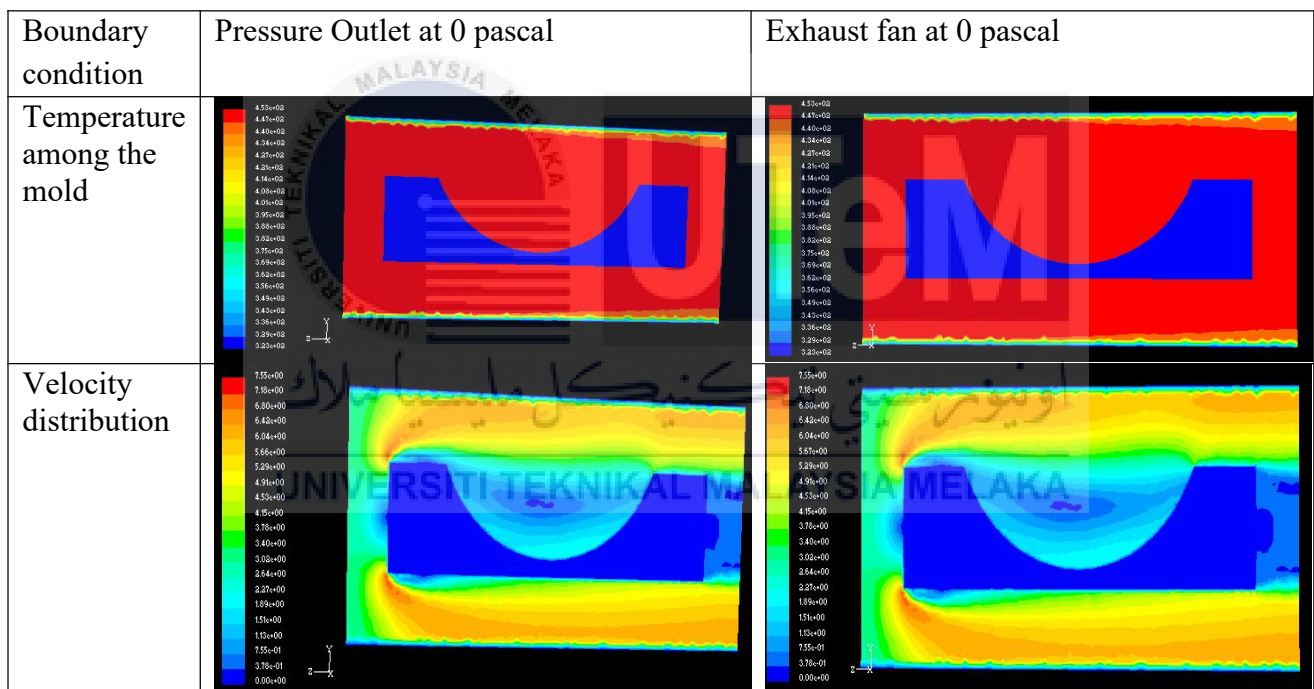


Figure 4.10: Comparison between boundary condition of pressure outlet and exhaust fan

From both results show in Figure 4.10, both show a similar flow pattern is observed. From a similar pattern, it meant that both boundary conditions that 0 pascal pressure outlet is the same as the exhaust fan at 0 pascals. The implement of the exhaust fan is to imitate the situation of suction of air to the air outlet. However, due to the exhaust fan located at the air outlet, which caused the increasing of time taken for simulation, yet the results gained are not in a converged condition. Therefore, pressure outlet is picked as the boundary condition that applied to the air outlet.



4.4 FLOW DISTRIBUTION AT DIFFERENT INLET VELOCITY

Figure 4.11 shows the flow distribution for 3 different models that are all similar in shapes, dimensions, and applied boundary conditions but different velocity are applied in the air flow of three models.

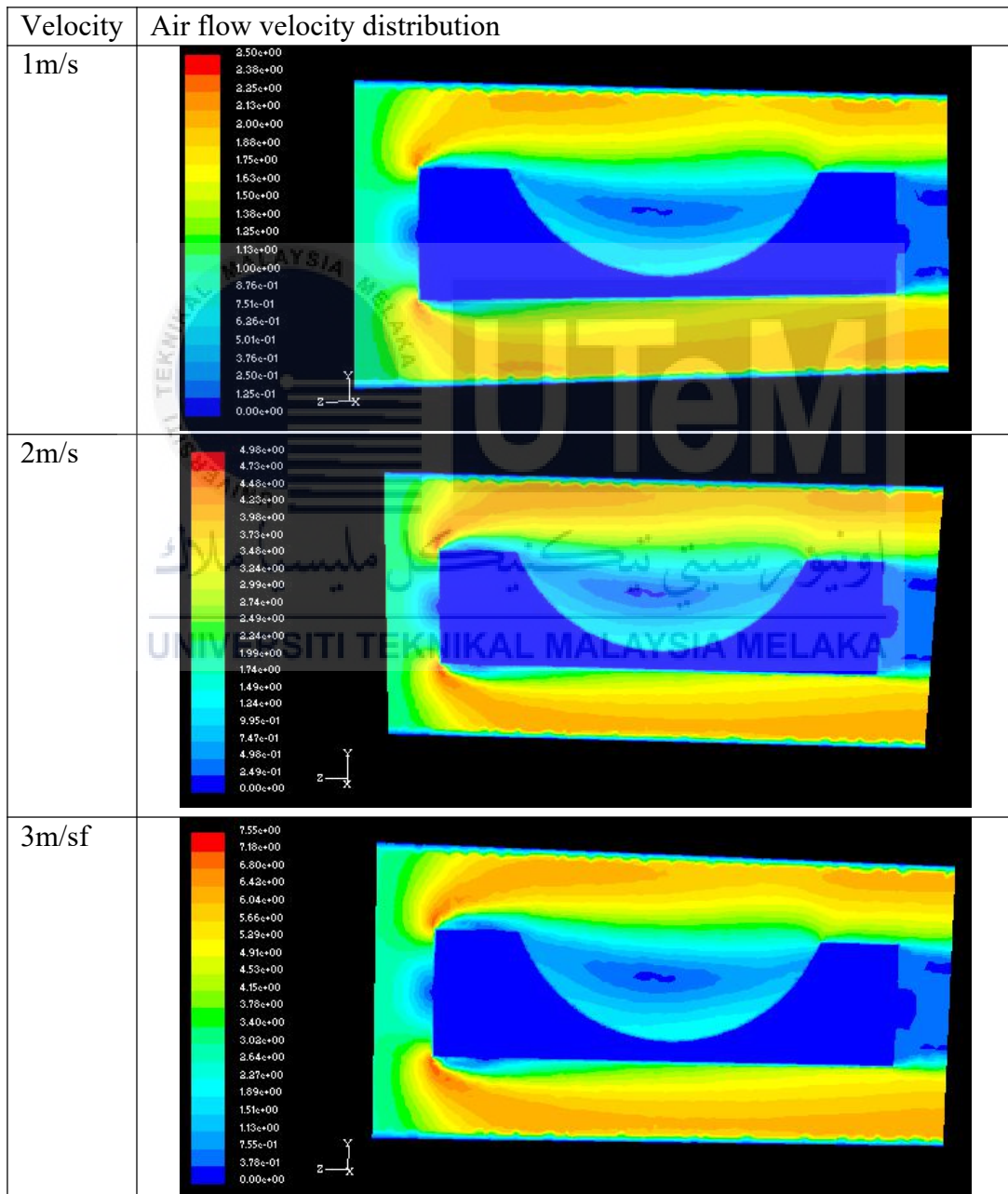


Figure 4.11: Velocity contour for inlet velocity of 1m/s, 2m/s, and 3m/s

From Figure 4.11, it has shown that for higher velocity inlet, velocity distribution increased as shown in 3 different cases. It is suspected that due to the limited occupied space with a high-speed air that flow through, the results are predicted similar but have some little difference at a certain point.

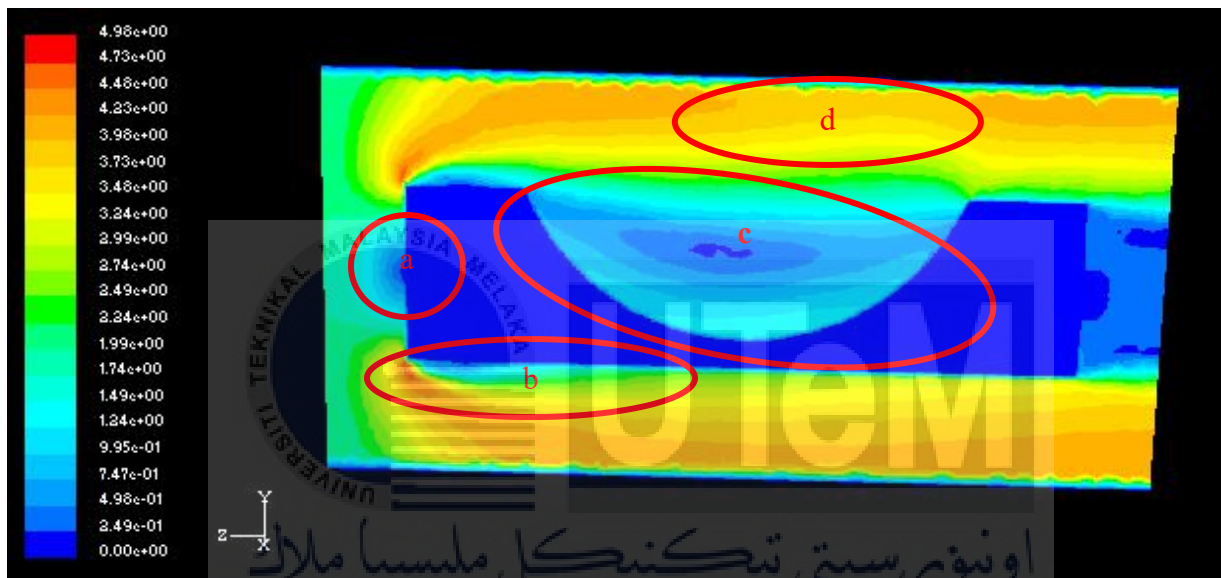


Figure 4.12: The red circles show the difference between three different cases

From Figure 4.12, Part a is due to the separation of airflow into up-and-down air flow that there is a stagnation point formed due to the reflect of air flow when hitting towards the solid mold. However, with higher velocity applied, the circulate air flow area will become smaller as shown in part c for each different velocity. Part b and d is due to boundary condition that at the nearest surface of solid, the velocity of air is approximated to zero. From the table 4x: the boundary layers formed differently with different velocity. The higher velocity will form a boundary layer which pulled longer than low velocity. The interesting part is part c where the

panel should place onto the mold and cure through the hot air. Part c is considered as a stagnation point that all heat is trapped surrounding the point which helpful for the curing process. With the higher velocity applied, the more uniform the circulating velocity for the trapped air which helps to heat up or cure the panel faster.



4.5 TEMPERATURE DISTRIBUTION AT DIFFERENT VELOCITY

Figure 4.13 is the table for the temperature distribution that obtained from three different models with a velocity of air inlet about 1m/s, 2m/s, and 3m/s. From Figure 4.13, it can be clearly shown that the temperature of the air flow is observed to be uniform. These results indicate that the heat of air flow is able to spread on the surface of mold completely. However, due to the heated air that flow too fast, the heating process might take a longer time for that material which have to cure completely of inner to the outer surface.



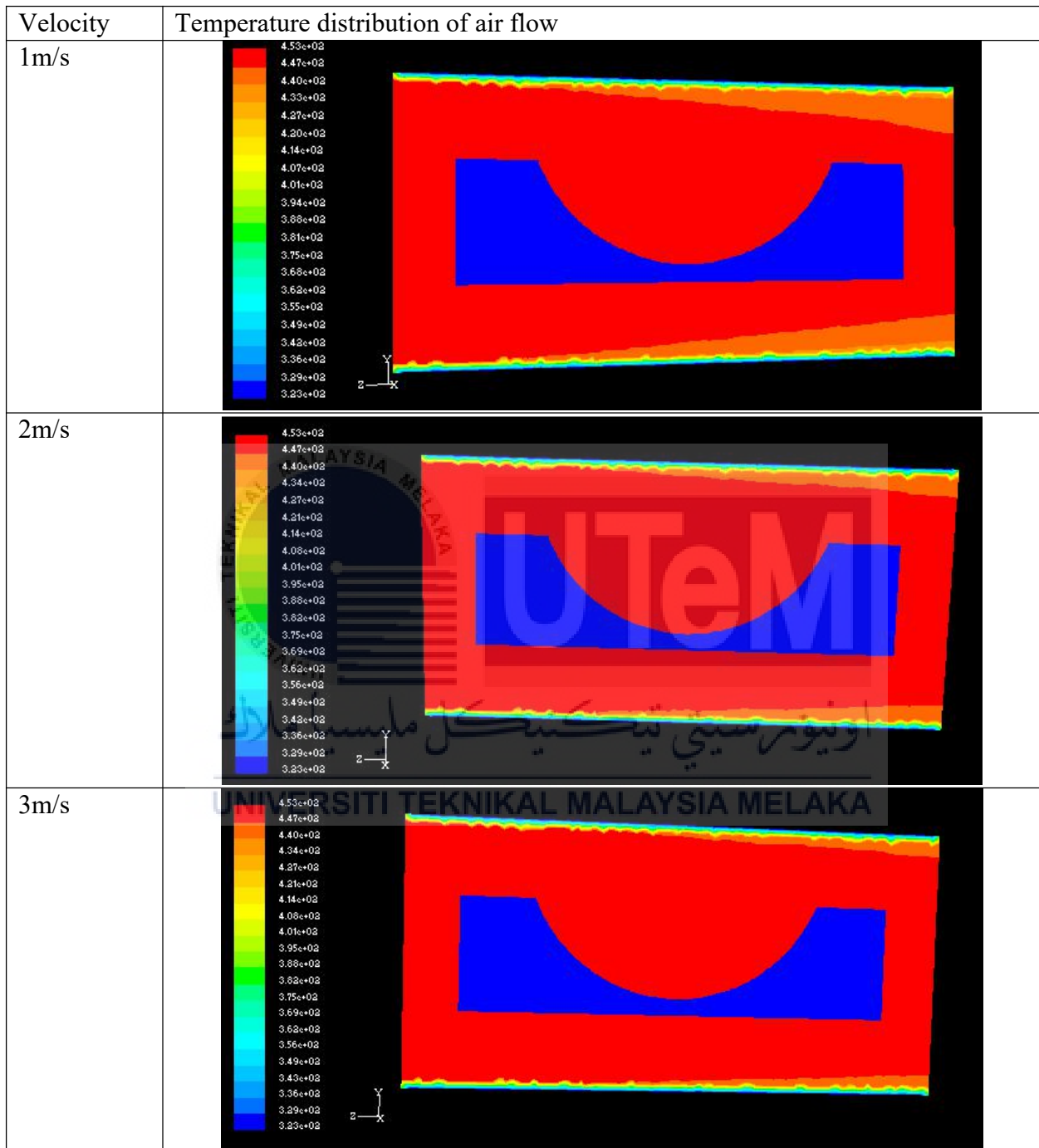
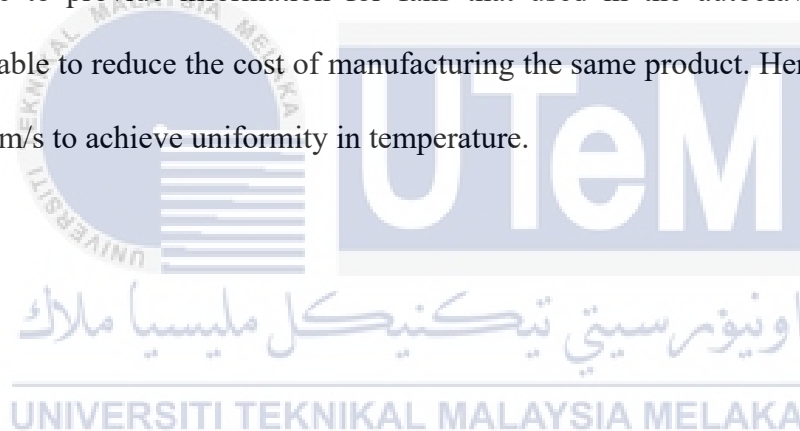


Figure 4.13: Temperature contour of air inlet velocity of 1m/s, 2m/s, and 3m/s

Furthermore, to obtain a suitable range of velocity for air flow through the autoclave chamber, a simple comparison between three different inlet velocities is made up which is 0.2m/s, 0.5m/s, and 1m/s.

From the Figure 4.14, the lower the velocity of heated air, the pattern of airflow starting to bend upward which followed the behavior of hot air flow upward while cold air flow downwards. However, the non-uniform pattern air flow that caused by low velocity has made the heating process on the surface of the mold become unevenly. Therefore, the range of velocity for uniform hot air flow is around 0.5m/s to 1m/s. The aim of the comparison is to obtain a range of velocity that able to provide information for fans that used in the autoclave to a minimum requirement that able to reduce the cost of manufacturing the same product. Hence, the minimum inlet velocity is 1m/s to achieve uniformity in temperature.



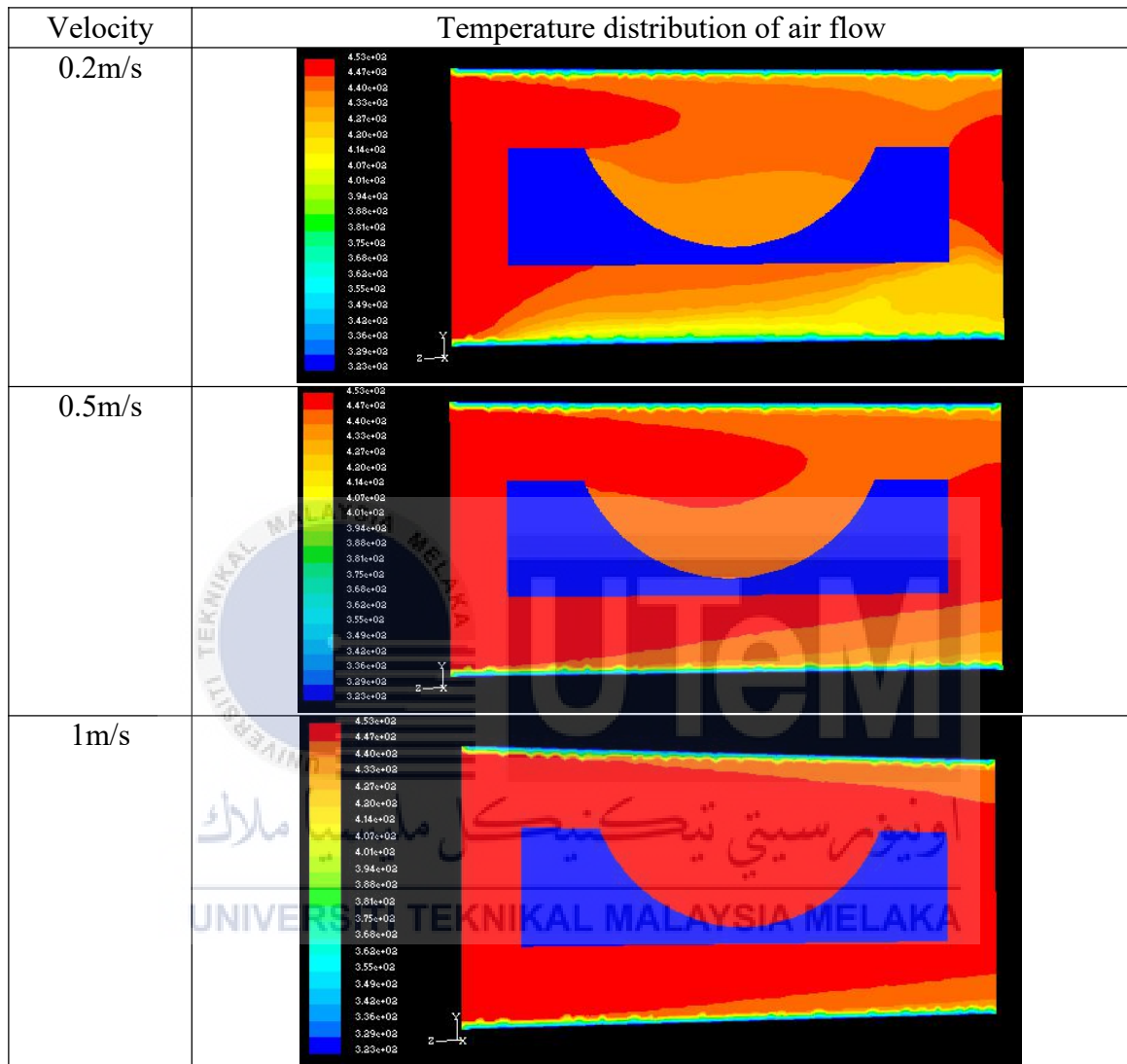


Figure 4.14: Temperature contour of air inlet velocity of 0.2m/s, 0.5m/s, and 1m/s

CHAPTER 5

CONCLUSION

The study of this project is to investigate the airflow inside the autoclave, which aim for further improvement of the autoclave. Throughout the simulation of the inner air flow of autoclave, there are several cases for velocity and temperature distribution. To modify the validation, there are three different models made for try and error. The model which has meshed with the highest number which is the third model is used for further simulation. However, the model with the panel is removed due to the skewness problem that occurred during the volumetric meshing of the particular model.

To illustrate the condition inside the autoclave where the air outlet is an area that the air is sucked out and moved into the air circulating system, the boundary condition used on air outlet are pressure outlet and exhaust fan, both are set at 0 pascals during the application. From the data gained, both are showing a similar result that indicates both conditions are applicable once the pressure gauge value is set. However, the exhaust fan condition is harder to gain results compared to the boundary condition of the pressure outlet that illustrates the outside atmosphere.

The velocity distribution of the air flow has shown that the stagnation point occurred at a needed location which is the middle part of the mold where the panel should be placed onto it and cure during the whole process. However, the higher the velocity of the air, the lesser the time that hot air is in-contacted with the surface that needs to cure, so it is not logic that applying high-speed hot air to cure a material from inner completely.

The temperature distribution shows that the difference in the pattern of hot air flow through the autoclave chamber. From the comparison, the lower the velocity, the heat inside of air flow becomes a non-uniform state that affects the efficiency of the curing process. To maximize the efficiency of the fan used, several simulations are made to identify the range of velocity of hot air that flows inside the autoclave. Throughout the simulations, the range of suitable velocity that should be applied is about 0.5m/s to 1m/s to ensure the surface of material that place on the mold is able to be cured or heated up in a short time period.

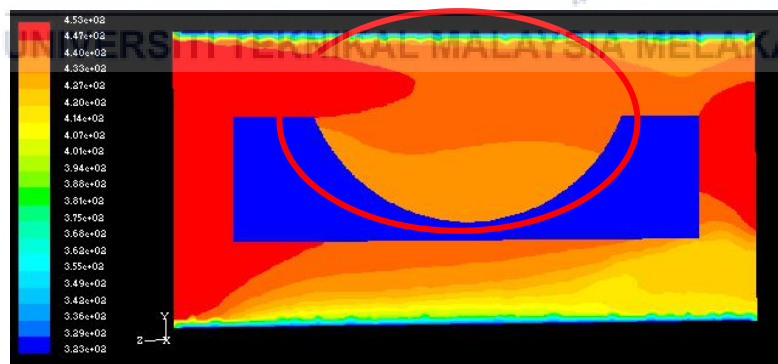


Figure 5.1: The red circle is the predicted area that a heater should be located

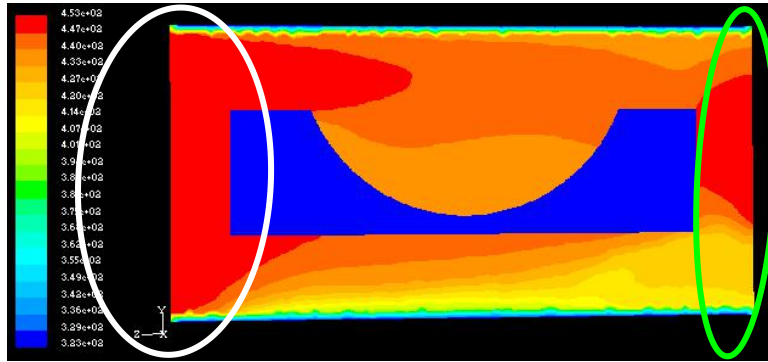


Figure 5.2: The white circle is the blower applied, while the green circle is the exhaust fan

Furthermore, the application of position on both fan and heater is determined through simulation. Two fans are located at both entrances of air inlet which represents as a blower that provides initial airflow and the exit of air outlet which considered as an exhaust fan that is used to suck out the airflow inside the autoclave chamber as shown in Figure 5.2. The heater is placed at a location that aims to increase the temperature of the airflow in that particular as shown in Figure 5.1. However, through the contour result obtained from the simulation, the suitable heater location should be placed at the upper part of the autoclave chamber region. The hot spot area which is the stagnation point location is determined. Therefore, the third objective is also achieved.

5.2 RECOMMENDATION

To improve the simulation, the smaller the size of meshing should be used. The smaller the meshing is, the better the result should obtain, but in a price that took a long time for running the simulation. However, to simplify the meshing process, with the using of ANSYS, all the meshing process are simplified. Other than that, the velocity of inner air flow should readjust to a certain scale to improve the time taken for simulation to run through. Furthermore, the lack of suitable journal that able to reference that has made this project hard to be done. The study about the autoclave inner air flow which in-related to the usage of CFD simulation is less and most of the results and research are kept as company secrets that hard to access.



REFERENCE

1. Burlon, F. *et al.* (2017) 'Transient model of a Professional Oven', *Energy Procedia*. Elsevier B.V., 126, pp. 2–9. doi: 10.1016/j.egypro.2017.08.045.
2. Chen, F., Zhan, L. and Xu, Y. (2014) 'Modelling and simulation for temperature distribution of mold during autoclave forming process', *Proceedings of the 12th International Conference on Heat Transfer, Thermal Engineering and Environment*, pp. 80–88.
3. Holman, M. C. (1989) 'Autoclave age forming large aluminum aircraft panels', *Journal of Mechanical Working Technology*, 20(C), pp. 477–488. doi: 10.1016/0378-3804(89)90055-7.
4. Illés, B. and Bakó, I. (2014) 'Numerical study of the gas flow velocity space in convection reflow oven', *International Journal of Heat and Mass Transfer*, 70, pp. 185–191. doi: 10.1016/j.ijheatmasstransfer.2013.10.075.
5. Kokolj, U., Škerget, L. and Ravnik, J. (2017) 'A numerical model of the shortbread baking process in a forced convection oven', *Applied Thermal Engineering*, 111, pp. 1304–1311. doi: 10.1016/j.applthermaleng.2016.10.031.
6. Lucchi, M. and Lorenzini, M. (2019) 'Control-oriented low-order models for the transient analysis of a domestic electric oven in natural convective mode', *Applied Thermal Engineering*. Elsevier Ltd, 147, pp. 438–449. doi: 10.1016/j.applthermaleng.2018.10.104.
7. Park, S. H. *et al.* (2018) 'Numerical study on the effect of different hole locations in the fan case on the thermal performance inside a gas oven range', *Applied Thermal Engineering*, 137, pp. 123–133. doi: 10.1016/j.applthermaleng.2018.03.087.

8. Ramaswamy Setty, J. *et al.* (2011) 'Autoclaves for aerospace applications: Issues and challenges', *International Journal of Aerospace Engineering*, 2011. doi: 10.1155/2011/985871.
9. Weber, T. A. *et al.* (2016) 'A fast method for the generation of boundary conditions for thermal autoclave simulation', *Composites Part A: Applied Science and Manufacturing*. Elsevier Ltd, 88, pp. 216–225. doi: 10.1016/j.compositesa.2016.05.036.
10. Xu, Y. *et al.* (2017) 'Numerical simulation of temperature field in large integral panel during age forming process: Effect of autoclave characteristics', *Procedia Engineering*. Elsevier B.V., 207, pp. 269–274. doi: 10.1016/j.proeng.2017.10.773.
11. Yi, Y. *et al.* (2017) 'Improving the Curing Cycle Time through the Numerical Modeling of air Flow in Industrial Continuous Convection Ovens', *Procedia CIRP*. The Author(s), 63, pp. 499–504. doi: 10.1016/j.procir.2017.03.167.
12. Zeng, X. and Raghavan, J. (2010) 'Role of tool-part interaction in process-induced warpage of autoclave-manufactured composite structures', *Composites Part A: Applied Science and Manufacturing*. Elsevier Ltd, 41(9), pp. 1174–1183. doi: 10.1016/j.compositesa.2010.04.017.
13. Zheng, H. *et al.* (2014) 'Computational fluid dynamics simulations and experimental validation of macromixing and flow characteristics in low-density polyethylene autoclave reactors', *Industrial and Engineering Chemistry Research*, 53(38), pp. 14865–14875. doi: 10.1021/ie502551c.

APPENDIX

Week	W1	W2	W3	W4	W5	W6	W7	W8	W9	W10	W11	W12	W13	W14	W15	W16
Briefing About Title																
Preparing of Literature Review																
Progress Report Evaluation																
Model Simulation Set Up																
Final Result Report																
Seminar																